Paper 16 open access : Photocatalytic Degradation of Textile Orange 16 Reactive Dye by ZnO Nanoparticles Synthesized via Green Route Using Punica Granatum Leaf Extract

Full paper dapat dilihat di bagian bawah ini

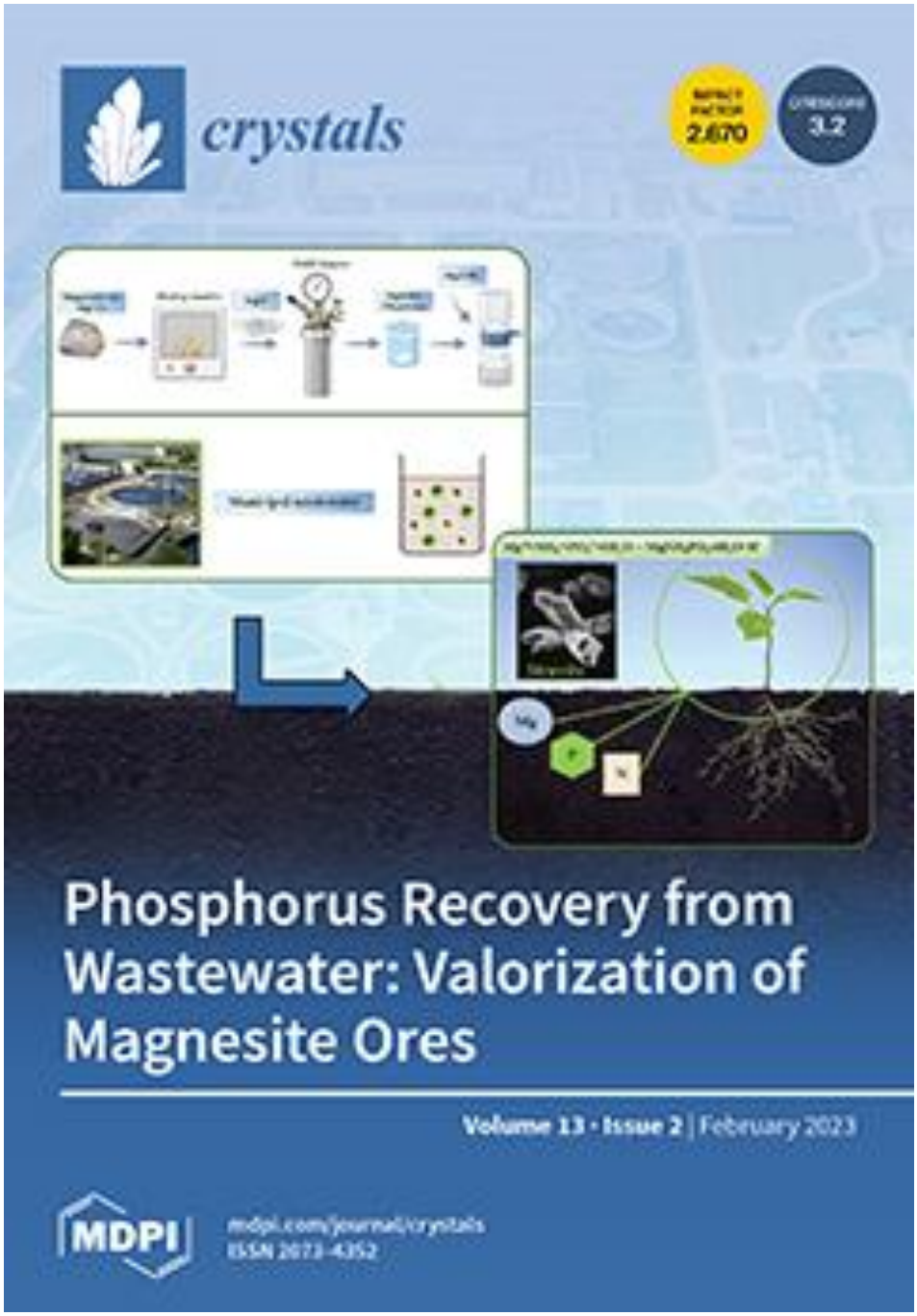

crystals

Submit to this Journal

Review for this Journal

Edit a Special Issue

Article Menu

Order Article Reprints

Open Access Article

Photocatalytic Degradation of Textile Orange 16 Reactive Dye by ZnO Nanoparticles Synthesized via Green Route Using Punica Granatum Leaf Extract

by Salma A. Al-Zahrani [1,*], Mallikarjunagouda B. Patil [2,*], Shridhar N. Mathad [3], Arun Y. Patil [4], Ahmed A. Otaibi [1], Najat Masood [1], Dorsaf Mansour [1], Anish Khan [5], A. Manikandan [6] and Edi Syafri [7]

https://www.mdpi.com/2073-4352/13/2/172

Members (515)

Search by first name, last name, affiliation, interest...

Prof. Dr. Helmut Cölfen Website

Editor-in-Chief

Physical Chemistry, Universität Konstanz, 78457 Konstanz, Germany

Interests: nucleation; nanoparticle self organization; non classical crystallization; mesocrystals; biomineralization; nanoparticle analysis by fractionating methods

Special Issues, Collections and Topics in MDPI journals

Prof. Dr. Hongbin Bei * Website

Section Editor-in-Chief

School of Materials Science and Engineering, Zhejiang University, Hangzhou 310000, China

Interests: alloy design and behavior; structural materials under extreme conditions; multiscale mechanical behaviors; physical metallurgy; metal and alloys; single crystals; plasticity

* Section: Crystalline Metals and Alloys

Special Issues, Collections and Topics in MDPI journals

Prof. Dr. Neil Champness Website

Section Editor-in-Chief

School of Chemistry, University of Nottingham, Nottingham, UK

Interests: supramolecular chemistry; crystal engineering; chemical nanoscience; molecular organisation from solid-state and solution-based self-assembly of nanoscale molecular architectures to success in surface molecular organisation

Special Issues, Collections and Topics in MDPI journals

Prof. Dr. Sławomir Grabowski Website

Section Editor-in-Chief

Kimika Fakultatea, Euskal Herriko Unibertsitatea UPV/EHU, Donostia International Physics Center (DIPC), P.K. 1072, 20080 Donostia, Euskadi, Spain

Interests: hydrogen bond; Lewis acid–Lewis base interactions; atoms in molecules theory; ab initio calculations

Special Issues, Collections and Topics in MDPI journals

Prof. Dr. Robert F. Klie **Website**

Section Editor-in-Chief

Department of Physics, University of Illinois at Chicago, Chicago, IL 60607, USA

Interests: transmission electron microscopy; scanning transmission electron microscopy; electron energy-loss spectroscopy; correlated oxides; molecular beam epitaxy; electron beam diffraction; magnetism

Special Issues, Collections and Topics in MDPI journals

Prof. Dr. Leonid Kustov **Website**

Section Editor-in-Chief

1. National University of Science and Technology «MISIS», 119049 Moscow, Russia
2. Department of Chemistry, M. V. Lomonosov Moscow State University, 119992 Moscow, Russia
3. N. D. Zelinsky Institute of Organic Chemistry, Russian Academy of Sciences, 119991 Moscow, Russia

Interests: catalysis; nanomaterials; renewables; green chemistry

Special Issues, Collections and Topics in MDPI journals

Prof. Dr. Heike Lorenz **Website**

Section Editor-in-Chief

Max Planck Institute for Dynamics of Complex Technical Systems, 39106 Magdeburg, Germany

Interests: phase equilibria; crystallization kinetics; process monitoring & design; separation of fine chemicals, large scale industrial products and renewable resources; innovative crystallization-based separation concepts; enantiomers; natural products; multi-component mixtures

Special Issues, Collections and Topics in MDPI journals

Prof. Dr. Abel Moreno **Website**

Section Editor-in-Chief

Instituto de Química, Universidad Nacional Autónoma de México. Av. Universidad 3000, Mexico Cd.Mx. 04510, Mexico

Interests: protein crystals; biocrystals; crystal growth; protein crystallography; crystal chemistry; biomineralization; biomimetics; biological macromolecules

Special Issues, Collections and Topics in MDPI journals

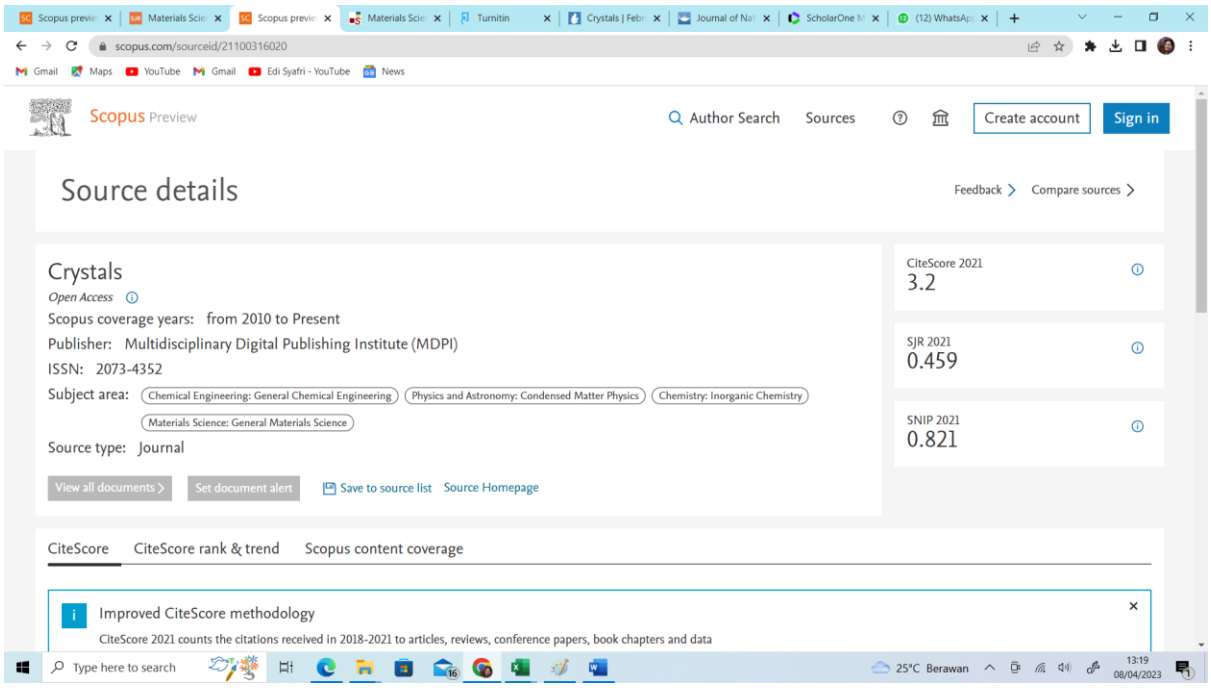

Crystals

COUNTRY

Switzerland

Universities and research institutions in Switzerland

Media Ranking in Switzerland

SUBJECT AREA AND CATEGORY

Chemical Engineering
- Chemical Engineering (miscellaneous)

Chemistry
- Inorganic Chemistry

Materials Science
- Materials Science (miscellaneous)

Physics and Astronomy
- Condensed Matter Physics

PUBLISHER

Multidisciplinary Digital Publishing Institute (MDPI)

H-INDEX

45

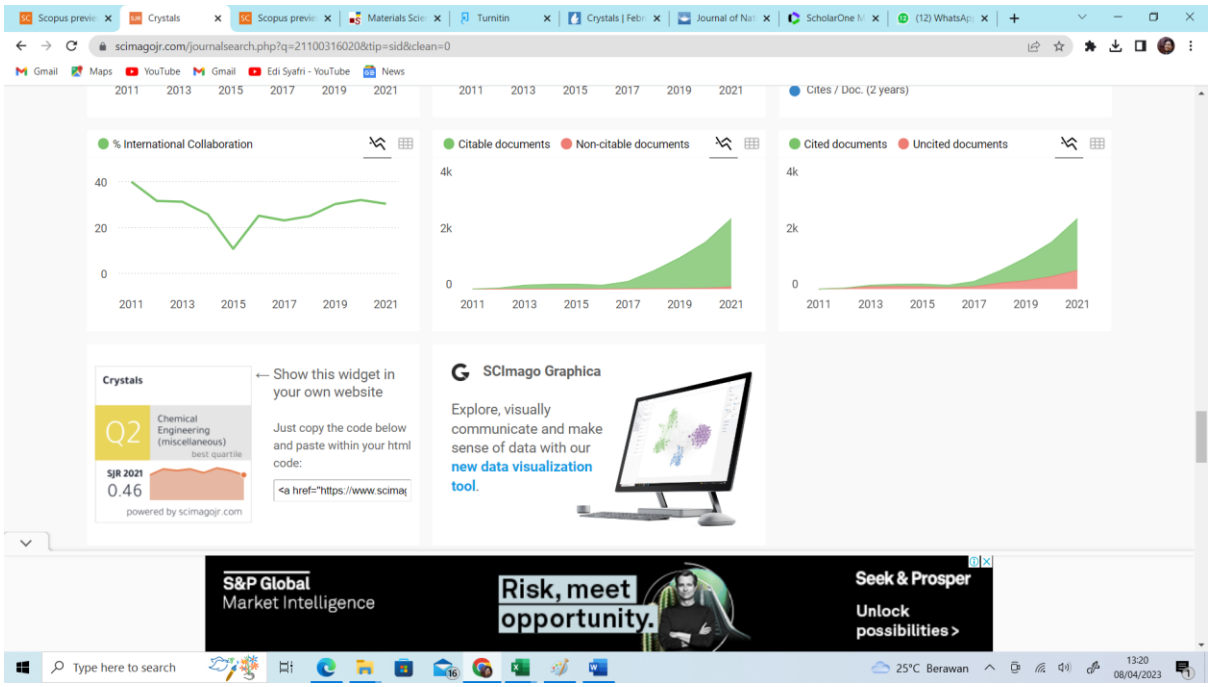

List of Contents

Volume 13, 2023 – issue 2

Open Access Article

Photocatalytic Degradation of Textile Orange 16 Reactive Dye by ZnO Nanoparticles Synthesized via Green Route Using Punica Granatum Leaf Extract

by Salma A. Al-Zahrani, Mallikarjunagouda B. Patil, Shridhar N. Mathad, Arun Y. Patil, Ahmed A. Otaibi, Najat Masood, Dorsaf Mansour, Anish Khan, A. Manikandan and Edi Syafri

Crystals **2023**, *13*(2), 172; **https://doi.org/10.3390/cryst13020172** - 18 Jan 2023

Cited by 1 | Viewed by 652

Abstract Since it does not use any dangerous chemicals and is a simple, low-cost process, the green synthesis approach for nanoparticle creation has several benefits compared to the physical and chemical synthesis routes. The current study describes an environmentally friendly synthesis of zinc oxide **[...] Read more.**

(This article belongs to the Special Issue Advanced Nanomaterials for Photocatalytic Technologies)

► **Show Figures**

Open Access Article

Mycosynthesis, Characterization of Zinc Oxide Nanoparticles, and Its Assessment in Various Biological Activities

by Asif Kamal, Malka Saba, Khetab Ullah, Saeedah Musaed Almutairi, Bandar M. AlMunqedhi and Mohamed Ragab abdelGawwad

Crystals **2023**, *13*(2), 171; **https://doi.org/10.3390/cryst13020171** - 18 Jan 2023

Cited by 1 | Viewed by 736

Abstract In recent years, nanotechnology has become one of the emerging fields of nanoparticle synthesis using biological processes. The use of mushroom extract is one of the most important methods for biological synthesis due to the presence of abundant biologically active compounds. In this **[...] Read more.**

(This article belongs to the Special Issue **Preparation and Antibacterial Properties of Metal Nanoparticles**)

► **Show Figures**

Open Access Article

Pressure-Induced Structural Phase Transitions in the Chromium Spinel $LiInCr_4O_8$ with Breathing Pyrochlore Lattice

by Meera Varma, Markus Krottenmüller, H. K. Poswal and C. A. Kuntscher

Crystals **2023**, *13*(2), 170; **https://doi.org/10.3390/cryst13020170** - 18 Jan 2023

Viewed by 598

Abstract This study reports high-pressure structural and spectroscopic studies on polycrystalline cubic chromium spinel compound $LiInCr_4O_8$. According to pressure-dependent X-ray diffraction measurements, three structural phase transitions occur at ~14 GPa, ~19 GPa, and ~36 GPa. The first high-pressure phase is **[...] Read more.**

(This article belongs to the Special Issue **Pressure-Induced Phase Transformations (Volume II)**)

► **Show Figures**

Open Access Review

Pure and Yb-Doped $La_xY_ySc_{4-x-y}(BO_3)_4$ Crystals: A Review of Recent Advances

by Alin Broasca, Madalin Greculeasa, Flavius Voicu, Cristina Gheorghe and Lucian Gheorghe

Crystals **2023**, *13*(2), 169; **https://doi.org/10.3390/cryst13020169** - 18 Jan 2023

Viewed by 444

Abstract This paper reviews the progress in developing the $La_xY_ySc_{4-x-y}(BO_3)_4$-LYSB and Yb-doped $La_xY_ySc_{4-x-y}(BO_3)_4$-LYSB:Yb huntite-type crystals grown by the Czochralski method as new candidates for **[...] Read more.**

(This article belongs to the Special Issue **Emerging Rare-Earth Doped Materials**)

► **Show Figures**

Open Access Article

Investigation of OP-GaP Grown on OP-GaAs Templates Using Nondestructive Reciprocal Space Mapping

by Balaji Manavaimaran, Axel Strömberg, Vladimir L. Tassev, Shivashankar R. Vangala, Myriam Bailly,

Open Access Article

Preparation and Properties of RDX@FOX-7 Composites by Microfluidic Technology

by Jin Yu, Hanyu Jiang, Siyu Xu, Heng Li, Yiping Wang, Ergang Yao, Qing Pei, Meng Li, Yang Zhang and Fengqi Zhao

Crystals **2023**, *13*(2), 167; **https://doi.org/10.3390/cryst13020167** - 18 Jan 2023

Viewed by 1116

Abstract 1,3,5-trinitro-1,3,5-triazacyclohexane (RDX) is a type of high energy explosive, its application in weapon systems is limited by its high mechanical sensitivity. At the same time, 1,1-diamino-2,2-dinitroethylene (FOX-7) is a famous insensitive explosive. The preparation of RDX@FOX-7 composites can meet the requirements, high energy **[...] Read more.**

(This article belongs to the Special Issue **Advanced Energetic Materials: Testing and Modeling**)

► **Show Figures**

Open Access Editorial

Emerging Low-Dimensional Materials (Volume I)

by Bo Chen, Rutao Wang and Nana Wang

Crystals **2023**, *13*(2), 166; **https://doi.org/10.3390/cryst13020166** - 18 Jan 2023

Viewed by 590

Abstract We recently published the first volume of the Special Issue "Emerging Low-Dimensional Materials" [...] **Full article**

(This article belongs to the Special Issue **Emerging Low-Dimensional Materials**)

Open Access Article

Ab Initio Theoretical Study of $DyScO_3$ at High Pressure

by Enrique Zanardi, Silvana Radescu, Andrés Mujica, Plácida Rodríguez-Hernández and Alfonso Muñoz

Crystals **2023**, *13*(2), 165; **https://doi.org/10.3390/cryst13020165** - 17 Jan 2023

Viewed by 499

Abstract $DyScO_3$ is a member of a family of compounds (the rare-earth scandates) with exceptional properties and prospective applications in key technological areas. In this paper, we study theoretically the behavior of $DyScO_3$ perovskite under pressures

crystals

MDPI

Article

Photocatalytic Degradation of Textile Orange 16 Reactive Dye by ZnO Nanoparticles Synthesized via Green Route Using Punica Granatum Leaf Extract

Salma A. Al-Zahrani [1,*], Mallikarjunagouda B. Patil [2,*], Shridhar N. Mathad [3], Arun Y. Patil [4], Ahmed A. Otaibi [1], Najat Masood [1], Dorsaf Mansour [1], Anish Khan [5], A. Manikandan [6] and Edi Syafri [7]

[1] Chemistry Department, Faculty of Science, University of Ha'il, P.O. Box 2440, Ha'il 81451, Saudi Arabia
[2] Bharat Ratna Prof. CNR Rao Research Centre, Basaveshwar Science College, Bagalkot 587101, Karnataka, India
[3] Department of Engineering Physics, K.L.E Institute of Technology, Hubballi 580027, Karnataka, India
[4] School of Mechanical Engineering, KLE Technological University, Vidya Nagar, Hubballi 580031, Karnataka, India
[5] Center of Excellence for Advanced Materials Research, King Abdulaziz University, Jeddah-21589, Saudi Arabia
[6] Department of Chemistry, Bharath Institute of Higher Education and Research (BIHER), Bharath University, Chennai-600073, Tamil Nadu, India
[7] Department of Agricultural Technology, Politeknik Pertanian Negeri Payakumbuh, West Sumatra 26271, Indonesia
* Correspondence: s.alzahrane@uoh.edu.sa (S.A.A.-Z.); mallupatil04@gmail.com (M.B.P.)

Abstract: Since it does not use any dangerous chemicals and is a simple, low-cost process, the green synthesis approach for nanoparticle creation has several benefits compared to the physical and chemical synthesis routes. The current study describes an environmentally friendly synthesis of zinc oxide (ZnO) nanoparticles (NPs) using an extract of *Punica granatum* plant leaves. Fourier-transform infrared spectroscopy (FTIR), ultraviolet-visible spectrophotometer (UV-Vis), field-emission scanning electron microscopy (FESEM), energy-dispersive X-ray spectroscopy, and X-ray diffraction techniques were used to characterize the morphology, composition, and structural properties of the synthesized zinc oxide nanoparticles. The XRD pattern reveals that the ZnO nanoparticles are crystalline and have a diameter of 20 nm. According to the FESEM studies, the ZnO-NPs have sizes ranging from 50 to 100 nm on average and are almost spherical. When exposed to direct sunlight, the produced ZnO-NPs demonstrate impressive photocatalytic oxidation of textile Orange 16, a reactive dye. As a result, our research advances the development of a green photocatalyst for the removal of harmful dyes from water.

Keywords: green synthesis; zinc oxide nanoparticle; photocatalytic; textile Orange 16 reactive dye

Citation: Al-Zahrani, S.A.; Patil, M.B.; Mathad, S.N.; Patil, A.Y.; Otaibi, A.A.; Masood, N.; Mansour, D.; Khan, A.; Manikandan, A.; Syafri, E. Photocatalytic Degradation of Textile Orange 16 Reactive Dye by ZnO Nanoparticles Synthesized via Green Route Using Punica Granatum Leaf Extract. *Crystals* **2023**, *13*, 172. https://doi.org/10.3390/cryst13020172

Academic Editor: Claudia Graiff

Received: 10 December 2022
Revised: 27 December 2022
Accepted: 13 January 2023
Published: 18 January 2023

1. Introduction

New nanoscale materials are being produced as a result of the advancements in nanotechnology. These materials have a variety of uses, including in consumer goods, nanomedicine, and nanoelectronics [1,2]. Because of their superior chemical and physical characteristics when compared to their bulk counterparts, research on such materials has increased significantly in recent years. Metal oxide nanostructures have been created, and they have a variety of uses in various industries. A semiconductor with a greater band gap (3.4 eV) is zinc oxide (ZnO). Applications for it include dye degradation, gas sensors, solar cells, and many others [3]. Numerous chemical and physical techniques, such as the sol–gel technique [4], the precipitation method [5], the arc discharge technique [6], the hydrothermal method [7], and the laser ablation method [8], have been adopted for the synthesis of ZnO nanoparticles. Due to its numerous advantages over the physical and

chemical approaches—including the fact that it does not use dangerous chemicals and is both environmentally friendly and economically advantageous—synthesis via the green method has been used to prepare ZnO nanoparticles [9,10]. This approach makes use of biological components that are readily available from plants.

Because they are readily available, leaves from the *Punica grantum* plant have been employed. The family of *Punicaceae*, which consists of two different species, is dominated by the pomegranate species (Punica granatum). *Punica grantum* plant leaves contain alkaloids, tannins, triterpenic acids, and flavonoids as phytochemicals [11]. Utilizing chemical reduction, these phytoconstituents produce metal oxide nanoparticles by acting as the stabilizing and reducing agents. As far as we are aware, there has not been any research on the usage of *P. granatum* leaves in the preparation of ZnO-NPs.

Organic substances called dyes are used in the paper, food, leather, and textile industries. Strongly colored, hazardous dyes are present in the effluents from these enterprises. The discharged effluents will enter running water, polluting the surface and groundwater and perhaps endangering the health of aquatic life as well as that of people, fauna, and the environment. Before release, the effluents would be treated to break down the dye into non-toxic species. Different purification methods, including chemical, biological, and physical techniques, have been developed, depending on the type of pollution. ZnO-NPs have been used to degrade dyes with success [12–14]. Through catalytic photooxidation with ZnO-NPs, reactive oxidative hydroxide radicals are created, which destroy the dyes. According to its chemical makeup, the textile Orange 16 reactive dye is an organic substance classified as a disulfonated triphenylmethane dye. Although originally designed for the textile industry, it is now frequently used for protein staining in biochemistry. The catalyst should be stable and reusable in addition to having a high degradation efficiency, as these qualities are crucial for industrial applications. Numerous investigations [15,16] have shown that ZnO-NPs are stable and reusable.

The *P. granatum* leaf extract was used in the current work's green synthesis to create ZnO-NPs. Under exposure to direct sunlight, the green ZnO-NPs that were generated were used to photocatalytically degrade the textile Orange 16 reactive dye.

2. Materials and Methodology

2.1. Materials

We gathered *Punica granatum* leaves from a field in Kaladagi near Bagalkot (India). Zinc nitrate hexahydrate of high purity was procured from Sigma-Aldrich, Mumbai, India. All water used in the experiment was deionized distilled water. We bought textile Orange 16 reactive dye from a local market in Bagalkot, Karnataka, India, through a textile business. None of the chemicals were further purified before use. Glassware washed in a prepared Piranha solution (3:1 volume ratio of H_2SO_4/H_2O_2) was rinsed with deionized (DI) water with a resistivity of 16.4 MΩ·cm (millipore water), dried in an oven, and returned for later use.

2.2. Methodology

2.2.1. Extraction of *Punica granatum* Leaf

Young *P. granatum* leaves were collected from a *Punica granatum* plantation at a Kaladagi village near Bagalkot (India). The leaves' middle rib was cut off. The leaves that remained were cleaned with distilled water to get rid of dust, and they were then dried in the shade to get rid of all the moisture. An aqueous extract of *Punica granatum* leaf was prepared. During the process, the dried leaves were weighed accurately and were finely grounded in a mixture. Then, deionized water was added to the dried fine powder. For about three hours, the mixture was refluxed at 60 °C, using the Soxhlet extractor apparatus. Once the green color turned brownish, the process was stopped. At room temperature, the solution was allowed to cool for the period of ten to fifteen minutes. Furthermore, Whatman No. 41 filter paper was used to filter the solution, and the filtrate was then

collected in a dry flask while the residue was thrown away. For future use, the leaf extract was kept at ambient temperature.

2.2.2. Green Synthesis of Zinc Oxide Nanoparticles (ZnO-NPs)

In deionized water, a solution of $Zn(NO_3)_2 \cdot 6H_2O$ (0.1 M) was made. The mixture was made homogeneously by stirring it without being heated. After that, a magnetic stirrer was used to gradually add drops of the aqueous leaf extract to the zinc nitrate solution. After the leaf extract was completely added, the resulting mixture was stirred with heating at 60 °C for 3–4 h on a hot plate until it took the form of slurry. The obtained slurry substance was filtered and placed in a crucible. The sample was calcined at 500 °C in a muffle furnace at a heating rate of 5 °C for 5 h. After calcination, white powder was obtained and stored properly.

2.2.3. Characterization of ZnO-NPs

A Siemens D 5000 (Malvern, UK) powder X-ray diffractometer was used to perform X-ray diffraction on the powdered zinc oxide nanoparticles. The UV-visible spectrum of the zinc oxide nanoparticles was recorded by employing a UV spectrophotometer (Systonic, Bangalore, India). The samples were evaluated between 200 and 800 nm. A Shimadzu (Model: IR Affinity-1, Tokyo, Japan) FTIR spectrometer was used to perform Fourier-transform spectroscopic measurements. A Carl Zeiss (Model: Sigma 300, Bangalore, India) field-emission scanning electron microscope (FESEM) was used to examine the surface morphology and the dimension of the particles of the prepared ZnO nanoparticles. The Oxford instrument (Buckinghamshire, UK), an energy-dispersive X-ray spectroscopy (EDX), was used to obtain the spectrum to check the purity of the synthesized ZnO nanoparticles and the stoichiometry of the samples. The particle size of the synthesized ZnO-NPs was determined using the Zetasizer (Model 3000HS, Malvern, UK). On a cuvette, the zeta average size of ZnO-NPs suspended in DI water was determined. The measurement was repeated three times, and the average value was used for data analysis.

2.2.4. Photocatalytic Activity of ZnO-NPs

A photodegradation study of textile Orange 16 reactive dye in water by exposure to sunlight was used to determine the ZnO nanoparticles as the photocatalysts. For this, an artificial, laboratory-simulated dye was prepared by dissolving the dye in water until the solution's absorbance value was more than one, i.e., 0.4 g in 100 mL of water. To the prepared colored mixture, a known amount of ZnO (i.e., 0.1 g), which would act as a photocatalyst, was added. Later, the aqueous solution was sonicated for 30 min. The solution was then kept in sunlight while being constantly stirred. After 30 min, 5 mL of the solution was withdrawn and centrifuged to settle down the ZnO photocatalyst. The supernatant solution was used to measure the absorbance with a UV-Vis spectrophotometer. From the experiment, it was observed that the value of absorbance reduced after each interval, showing the degradation of the dye by the ZnO-NPs. The detailed stepwise green synthesis of ZnO nanoparticles and their photocatalytic action are shown in Figure 1.

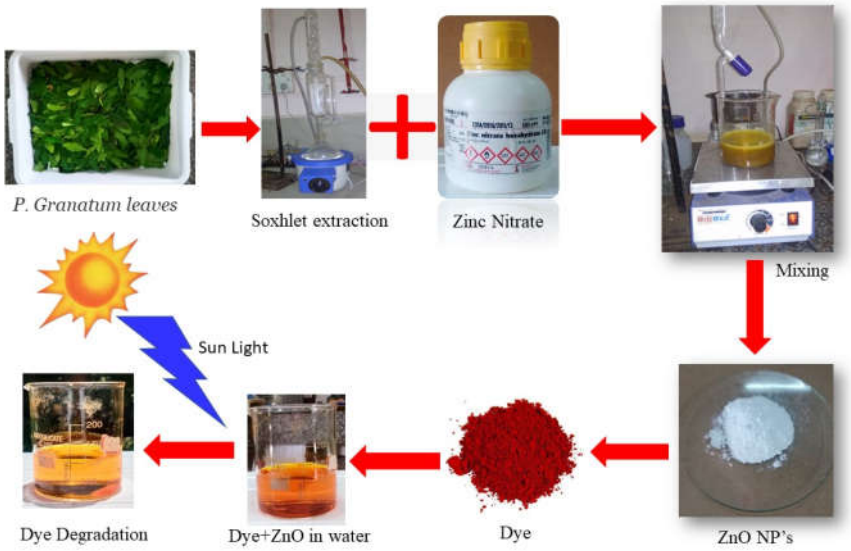

Figure 1. Step-by-step process of ZnO-NP synthesis via green route and the degradation of the dye.

3. Results and Discussion

3.1. X-ray Diffraction Analysis

Figure 2 depicts the X-Ray diffraction graph of the green synthesized ZnO nanoparticles. The sample was examined at various angles, ranging from 0° to 70°. ZnO nanoparticles have significant peaks at 2θ = 31.81°, 34.49°, 36.28°, 47.62°, 56.63°, 62.91°, and 68°, which can be designated as (100), (002), (101), (102), (110), (103), and (200), respectively. The orientation and crystallinity of the ZnO-NPs were revealed by using the X-ray pattern. The JCPDS data sheet/ICDD no. 36-1451 was used to compute the XRD pattern. The obtained X-ray pattern demonstrate that ZnO-NPs were synthesized using the green synthesis route, with the establishment of crystalline and wurtzite hexagonal structures. The particle dimension of ZnO-NPs was computed using the Debye–Scherrer equation from the highest peak (101) in the XRD graph:

$$d = \frac{K\lambda}{\beta cos\theta} \quad (1)$$

where d is the size of the crystallite; λ is the wavelength for diffraction; β is the corrected value of FWHM; θ is the angle of diffraction; and K is the universal and its value is near unity, i.e., 0.94.

The purity of the ZnO-NPs is confirmed by the absence of diffraction peaks from other phases.

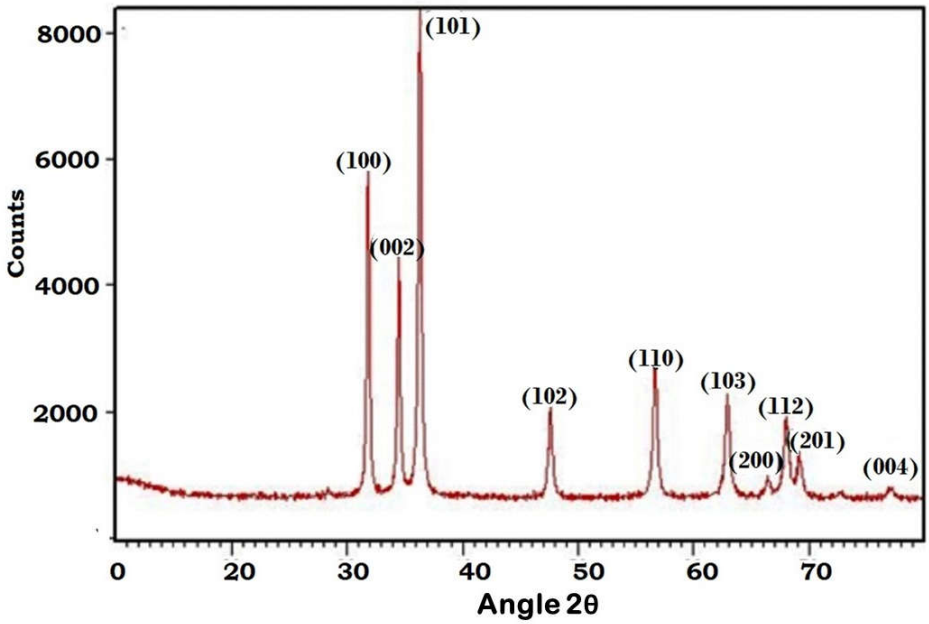

Figure 2. X-ray diffraction curves of green synthesized ZnO nanoparticles.

Bragg's equations 3-5 were used to calculate the inter-planar spacing (d), the lattice parameters (a = b and c) for the hexagonal wurtzite structure, and the volume of the hexagonal system unit cell (V) [17–20]. Table 1 summarizes all of these parameters.

$$n\lambda = 2d\ sin\ \theta \quad (2)$$

$$\frac{1}{d_{hkl}^2} = \frac{4}{3}\left(\frac{h^2 + hk + k^2}{a^2}\right) + \frac{l^2}{c^2} \quad (3)$$

$$V = \frac{\sqrt{3}}{2}a^2c \quad (4)$$

where d_{hkl} = inter-planar spacing; V = volume of the unit cell; and a, c = lattice parameters for the ZnO-NP.

Table 1. Crystallite size (D), inter-planar spacing (d), lattice parameters ($a = b$ and c), and volume (V) were calculated from the XRD measurements at 50 mmol/kg concentrations of $Zn(NO_3)_2{\cdot}6H_2O$.

[a]m (mmol/kg)	D (nm)	d (nm)	$a = b$ (nm)	c (nm)	V (nm^3)
50	31.158	0.256	0.325	0.527	4.721

[a]m represents the molality of $Zn(NO_3)_2{\cdot}6H_2O$ in water.

3.2. Particle Size Analysis

The particle size of the ZnO-NPs is depicted in Figure 3. The obtained results reveal that the size of ZnO particles ranges between 60 and 100 nm. The average particle size is measured at 80 nm.

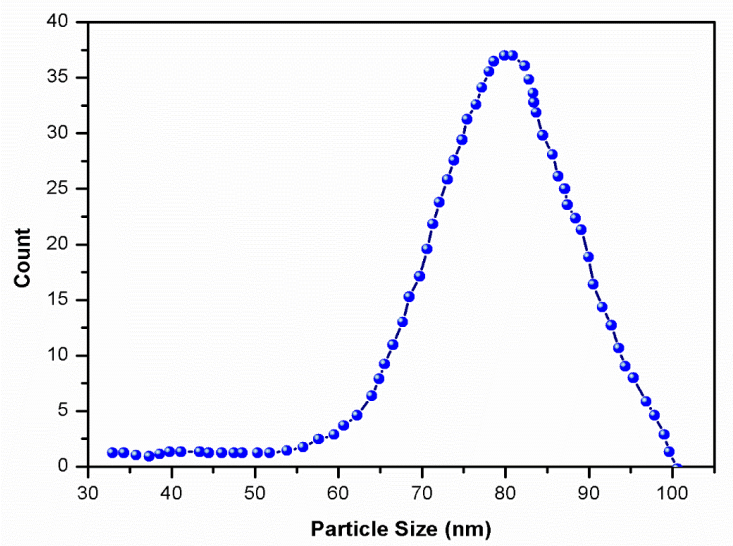

Figure 3. Histogram of ZnO particle size distribution.

3.3. UV-Visible Spectroscopic Analysis

Surface plasmon resonance distinguishes the absorbance pattern of nanoparticles from that of their bulk counterparts. The UV-visible measurement was used to confirm the formation of nanoparticles. Figure 4 depicts the UV-visible absorption spectrum of the ZnO-NPs. Using a systonic UV spectrophotometer, the substance was analyzed between 200 and 800 nm. The color of a solution of zinc nitrate hexahydrate ($Zn(NO_3)_2H_2O$) changed from white to brown when the *P. granatum* leaf extract was added. This resulted from the solution's synthesis of ZnO-NPs. The nanoparticles of zinc oxide are responsible for stimulating the surface plasmon vibrations, which in turn generate color changes. The absorbance peak was found to be centered at 382 nm, indicating that zinc nitrate hexahydrate had been converted to ZnO-NPs [21–23].

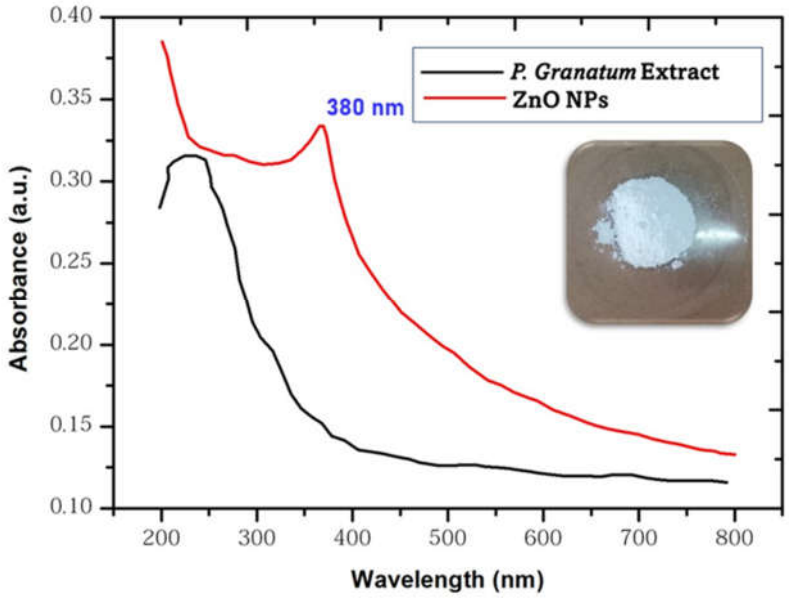

Figure 4. ZnO-NPs and *P. granatum* leave extract spectra measured using an UV-visible spectrophotometer. (Inside: photograph of ZnO-NPs synthesized via green method).

The optical energy band gap (E_g) was calculated using Formula (5), and the results are shown in Table 2.

$$E_g = \frac{hc}{\lambda} \quad (5)$$

From this formula, 'h' represents the Planck's constant (6.626×10^{-34} J s), 'c' corresponds to the velocity of light (the value is 3×10^8 m s^{-1}), and λ corresponds to the wavelength of the peak with the maximum intensity [24].

Table 2. λmax and energy band gap (E_g) results of ZnO-NPs at three different concentrations of zinc nitrate hexahydrate.

[a]**m (mmpl/kg)**	λ_{max} **(nm)**	E_g **(eV)**
5	381	3.436 ± 0.3
10	386	3.369 ± 0.4
50	390	3.361 ± 0.3

[a]m represents the molality of $Zn(NO_3)_2 \cdot 6H_2O$ in water.

The band gap values were calculated, and the results are nearly equivalent to 3.4 eV, which is consistent with previously reported values in the literature. Suresh et al. (3.33 eV) [25] and Hancock et al. (3.39 eV) [26] reported comparable band gap results. The variation in the shape and size of the ZnO-NPs may explain the difference in E_g with Zn $(NO_3)_2 \cdot 6H_2O$ concentration. In addition, a decrease in E_g values is attributed to an increase in ZnO particle size [27].

3.4. FESEM and EDX Analysis

ZnO may be produced into several nanostructures, including nanospheres, nanorods, and others. By looking at and analyzing each minute topographical feature using a field-emission scanning electron microscope (FESEM), the particle size and shape may be determined. The particle size and shape of the synthesized ZnO nanoparticles were analyzed with the aid of a Carl Zeiss FESEM. Figure 5 displays a FESEM picture of the ZnO nanoparticles that were synthesized via the green route. This image demonstrates that the particle is composed of nanostructures, which are even smaller structures. The XRD investigation indicated that the nanoparticles are fully spherical, with an average diameter of 80 nm.

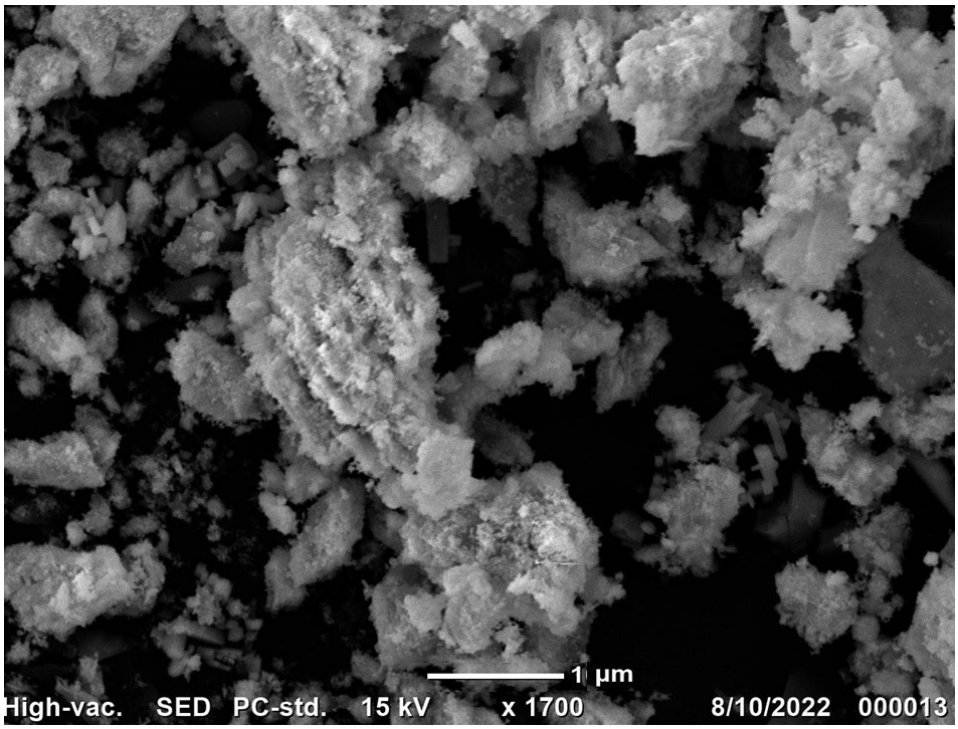

Figure 5. FESEM picture of zinc oxide NPs synthesized via the green route.

EDX was utilized to undertake an elemental investigation or chemical composition on the ZnO nanoparticles made in an environmentally responsible manner. The stoichiometry and chemical purity of the samples were analyzed using an EDX-equipped equipment from Oxford. The EDX spectrum of the ZnO nanoparticles is illustrated here in Figure 6. The EDX spectrum indicates indisputably that ZnO and oxygen (O) ions are present in the ZnO nanoparticles formed by the *P. Granatum* reaction. According to the findings of the elemental analysis, the ZnO powder is made up of 76% zinc and 15% oxygen, which shows that it is quite pure and only comprises a minor number of contaminants. The stoichiometry reveals that the mass percentages of zinc and oxygen should be 80.3% and 19.7%, respectively, if we are to trust the formulae.

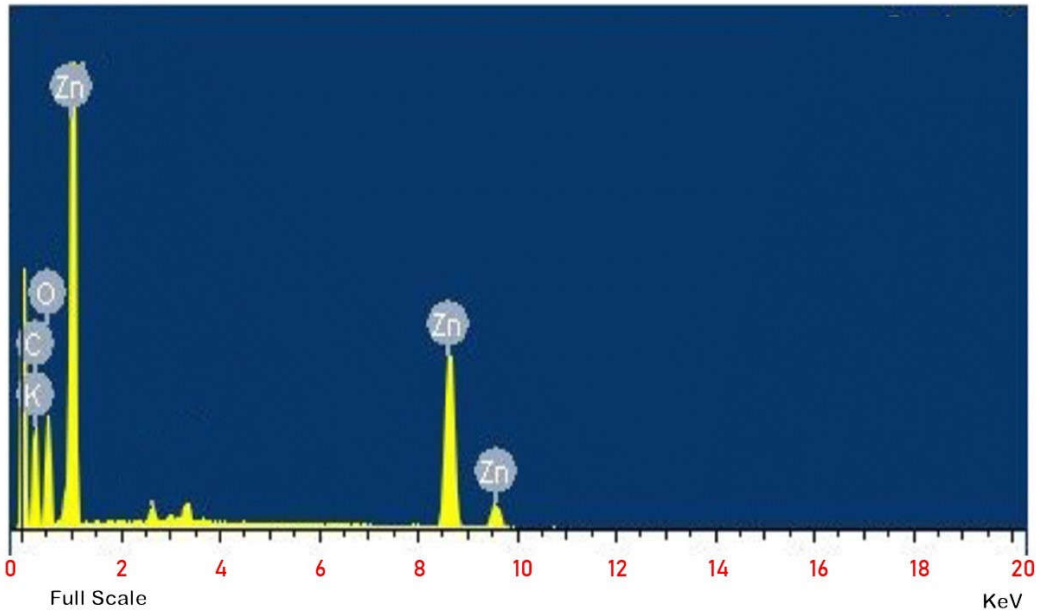

Figure 6. EDAX pattern for the green synthesized ZnO-NPs (Zn—zinc, O—oxygen, and C—carbon).

3.5. FT-IR Analysis

FT-IR spectroscopy was used to establish the presence of the Zn–O bond and its formation mechanism, as well as to detect the photo components that coat the surface of the ZnO-NPs. Fourier-transform infrared spectroscopy was performed using a Bruker Alpha FTIR as the instrument. Figure 7 depicts the FT-IR spectra of the ZnO-NPs that were synthetically generated via the green route. Both the 3610 cm^{-1} and 3822 cm^{-1} spectral peaks are the consequence of O–H stretching. The C–H stretch is responsible for the peak that appears at roughly 2354 cm^{-1}. The peak is induced by C=O stretching and is located at about 1512 cm^{-1}. There is a link between the peaks at 1635 cm^{-1} and ZnO vibrations caused by bending deformation. At 610 cm^{-1}, strong vibrational bands are produced as a result of the stretching modes utilized to form the ZnO nanoparticles. The phytoconstituents of P. granatum prevent the aggregation of ZnO-NPs during their production [22,23,28,29]. This is achieved by stabilizing the nanoparticles' surface.

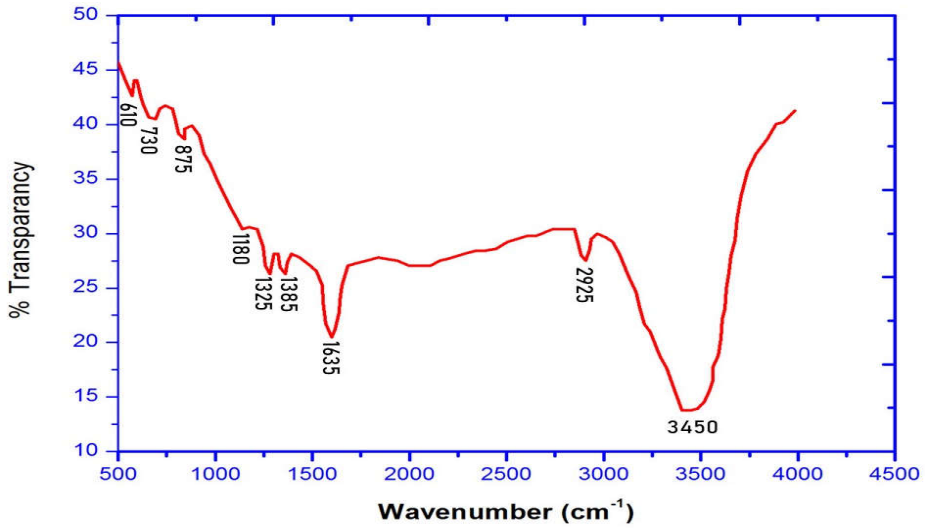

Figure 7. FTIR spectrum of ZnO-NPs.

3.6. Photocatalytic Activity

To evaluate the photodegradation of textile Orange 16 reactive dye in the presence of ZnO nanoparticles, the decrease in the absorbance of the dye was determined. The decrease in the absorbance of the dye solution as a function of exposure length is consistent with a decline in the concentration of textile Orange 16 reactive dye. Over time, the concentration of the blue pigment in the dye solution progressively lost its vibrancy, until it ultimately became light blue. Figure 8 depicts the deterioration of the textile Orange 16 reactive dye stain as a function of time in the samples exposed to sunlight. It can be seen that 600 nm is the wavelength at which textile Orange 16 reactive dye has the highest absorption peak. In addition, it reveals that ZnO-NPs are capable of significantly reducing the pollutant within three hours.

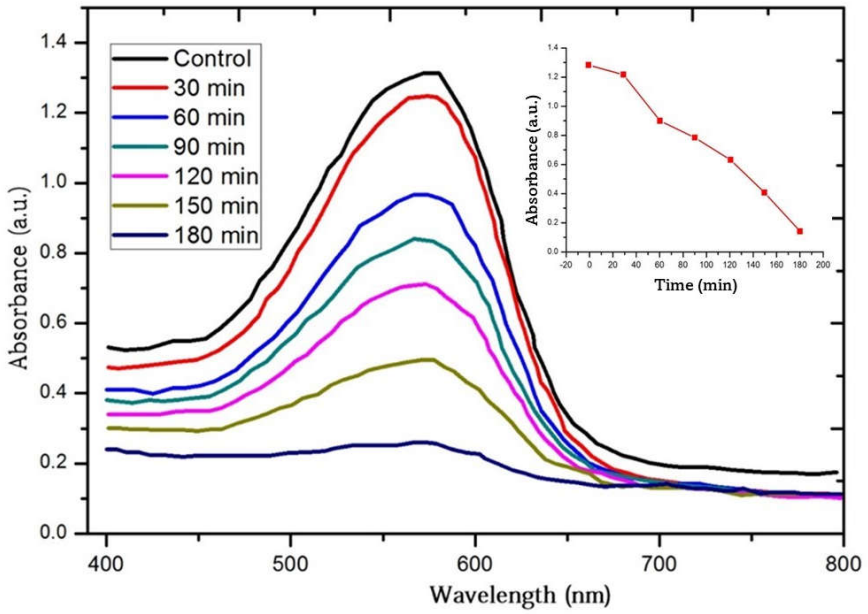

Figure 8. UV-vis absorption spectra showing the degradation of textile Orange 16 reactive dye by photocatalytic action using zinc oxide NPs synthesized via the green route at 30 min time intermissions. Inset: decrease in intensity of textile Orange 16 reactive dye in the presence of ZnO-NPs with time.

3.7. Recyclability and Photostability

Three cycles of photocatalysis were conducted to assess whether or not the photocatalyst could be recycled. The images are depicted in Figure 9. Figure 9a shows a 100% efficiency even after three cycles of photocatalysis. In addition, as seen in Figure 9b, the XRD measurements performed after the photocatalytic phenomenon show that the crystalline structure of ZnO has not altered when compared to before the photocatalytic process was undertaken.

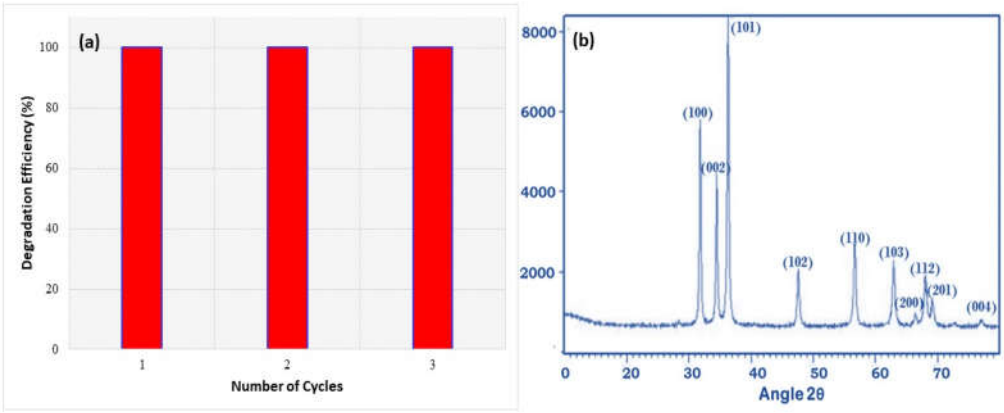

Figure 9. (**a**) The degradation profile of ZnO-NPs for three cycles and (**b**) XRD of ZnO after three cycles.

Figure 10 shows the photodegradation of the Orange 16 dye by using green synthesized ZnO nanoparticles. As observed in Figure 10, the effectiveness of the ZnO-NPs as photocatalysts for the breakdown of organic materials is shown by the decline in the color intensity of the dye with respect to the time of exposure to sunlight.

Figure 10. The color intensity before and after photodegradation using green synthesized ZnO nanoparticles.

3.8. Photolysis

There are three types of photocatalytic dye degradation mechanisms: (1) dye sensitization via charge injection, (2) indirect dye degradation via oxidation/reduction, and (3) direct photolysis of the dye. Photocatalytic substances are generally classified into three generations. One-component (e.g., ZnO and TiO_2) and multi-component semiconductor metal oxide (e.g., ZnO-TiO_2 and Bi_2O_3-ZnO) photocatalysts are classified as first-generation and second-generation, respectively. Third-generation photocatalysts are photocatalysts that are dispersed on an inert solid substrate (e.g., Ag-Al_2O_3 and ZnO-C).

Because some dyes are degraded by direct UV irradiation, it is necessary to investigate the extent to which textile Orange 16 reactive dye is photolyzed in the absence of a photocatalyst. In the absence of the photocatalyst, direct UV radiation exposure photolyzed textile Orange 16 reactive dye by up to 25% in 30 min. When ZnO-NPs were used as a photocatalyst and exposed to UV radiation, it was discovered that the

photodegradation of the dye increased by decolorizing the textile Orange 16 reactive dye with an efficiency of 96% in 30 min. The time-dependent photocatalytic degradation and the photolysis of textile Orange 16 reactive dye concentration are shown in Figure 11.

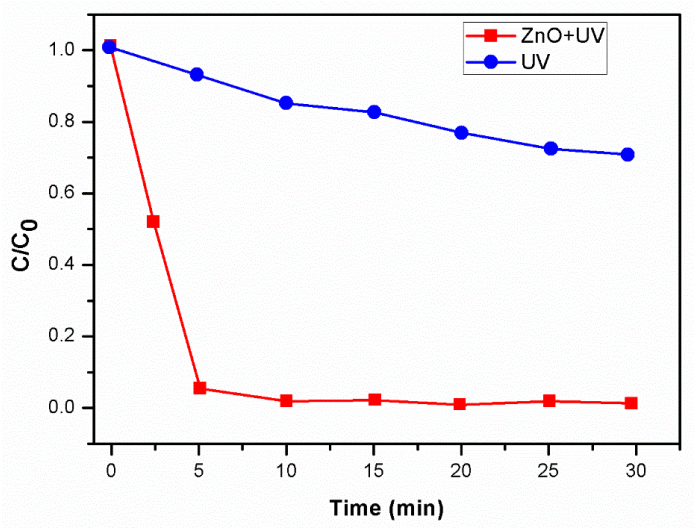

Figure 11. Time-dependent photocatalytic degradation and photolysis of textile Orange 16 reactive dye concentration (C/C_0).

3.9. Comparison

The dye photodegradation in the presence of the synthesized ZnO-NPs was compared to a commercial ZnO and previously reported work. The results are tabulated in Table 3.

Table 3. Comparison of ZnO-NPs as a photocatalyst for dye degradation.

Sl. No	Photocatalyst	Time (min)	% Photocatalytic Degradation of Dye	Reference
1	ZnO	180	94	Present work
2	ZnO	180	95	Commercial ZnO
3	ZnO	160	86.9	[17]

Among the tested ZnO NPs, commercial ZnO performed the best when compared to other ZnO NPs.

4. Conclusions

In the current investigation, an extract of the leaves of *P. granatum* was dissolved in water and utilized in a green synthesis process, which resulted in the successful generation of ZnO-NPs. The preparation of spherical, polydisperse ZnO-NPs with sizes ranging from 50 to 100 nm and an average size of 80 nm was performed. The majority of the nanoparticles are spherical and have an 80 nm diameter. According to the results of the EDX analysis, the ZnO powder has a very high degree of purity and includes nearly no impurities. The powder consists of 76% zinc and 15% oxygen. According to the results of the photocatalytic experiment, the bio-produced ZnO-NPs are able to photodegrade the textile Orange 16 reactive dye with an overall efficiency of 93%. The photolysis of the textile Orange 16 reactive dye concentration without and with ZnO-NPs shows that the ZnO-NPs play the role of photocatalysts effectively. According to the results of this work, the manufacture of ZnO-NPs using the *P. granatum* leaf extract is safe, inexpensive,

straightforward, and environmentally friendly, and these nanoparticles have shown efficacy as green photocatalysts in the actual treatment of wastewater.

Author Contributions: Conceptualization, S.A.A.-Z. and M.B.P.; methodology, S.N.M. and A.Y.P.; software, A.A.O; validation, N.M., D.M. and A.K.; formal analysis, A.M.; investigation, E.S.; project administration, S.A.A.-Z. All authors have read and agreed to the published version of the manuscript.

Funding: This research has been funded by Scientific Research Deanship at the University of Ha'il-Saudi Arabia through project number RG-21 032.

Data Availability Statement: Data can be provided on the request from the corresponding author.

Acknowledgments: Author are thankful for VGST, Bangalore, India for the support.

Conflicts of Interest: The authors declare no conflict of interest.

References

1. Saini, R.; Saini, S.; Sharma, S. Nanotechnology: The future medicine. *J. Cutan. Aesthetic Surg.* **2010**, *3*, 32. https://doi.org/10.4103/0974-2077.63301.
2. Singh, A. Synthesis, characterization, electrical and sensing properties of ZnO nanoparticles. *Adv. Powder Technol.* **2010**, *21*, 609–613.
3. Nohavica, D.; Gladkov, P. ZnO nanoparticles and their applications—New achievments. *NANOCON* **2010,** *1,* 121–124. https://doi.org/10.1016/j.cej.2012.01.076.
4. Azlina, H.N.; Hasnidawani, J.N.; Norita, H.; Surip, S.N. Synthesis of SiO_2 nanostructures using sol-gel method. *Acta Phys. Pol. A* **2016**, *129*, 842–844.
5. Raoufi, D. Synthesis and microstructural properties of ZnO nanoparticles prepared by precipitation method. *Renew Energy* **2013**, *50*, 932–937. https://doi.org/10.1016/j.renene.2012.08.076.
6. Ashkarran, A.A.; Irajizad, A.; Mahdavi, S.M.; Ahadian, M.M. ZnO nanoparticles prepared by electrical arc discharge method in water. *Mater. Chem. Phys.* **2009**, *118*, 6–8. https://doi.org/10.1016/j.matchemphys.2009.07.002.
7. Aneesh, P.M.; Vanaja, K.A.; Jayaraj, M.K. Synthesis of ZnO nanoparticles by hydrothermal method. In *Nanophotonic Materials IV*; SPIE: Bellingham, WA, USA, 2007.
8. Singh, S.C.; Gopal, R. Synthesis of colloidal zinc oxide nanoparticles by pulsed laser ablation in aqueous media. *Phys. E Low-Dimens. Syst. Nanostructures* **2008**, *40*, 724–730. https://doi.org/10.1016/j.physe.2007.08.155.
9. Singh, J.; Kumar, S.; Alok, A.; Upadhyay, S.K.; Rawat, M.; Tsang, D.C.; Bolan, N.; Kim, K.H. The potential of green synthesized zinc oxide nanoparticles as nutrient source for plant growth. *J. Clean. Prod.* **2019**, *214*, 1061–1070. https://doi.org/10.1016/j.jclepro.2019.01.018.
10. Singh, J.; Dutta, T.; Kim, K.H.; Rawat, M.; Samddar, P.; Kumar, P. 'Green' synthesis of metals and their oxide nanoparticles: Applications for environmental remediation. *J. Nanobiotechnol.* **2018**, *16*, 84. https://doi.org/10.1186/s12951-018-0408-4.
11. Wang, R.; Ding, Y.; Liu, R.; Xiang, L.; Du, L. Pomegranate: Constituents, bioactivities and pharmacokinetics. *Fruit Veg. Cereal Sci. Biotechnol.* **2010**, *4*, 77–87.
12. Hassan, S.S.M.; Azab, W.I.M.E.; Ali, H.R.; Mansour, M.S.M. Green synthesis and characterization of ZnO nanoparticles for photocatalytic degradation of anthracene. *Adv. Nat. Sci. Nanosci. Nanotechnol.* **2015**, *6*, 045012. https://doi.org/10.1088/2043-6262/6/4/045012.
13. Bhuyan, T.; Mishra, K.; Khanuja, M.; Prasad, R.; Varma, A. Biosynthesis of zinc oxide nanoparticles from Azadirachta indica for antibacterial and photocatalytic applications. *Mater. Sci. Semicond. Process.* **2015**, *32*, 55–61. https://doi.org/10.1016/j.mssp.2014.12.053.
14. Davar, F.; Majedi, A.; Mirzaei, A. (2015) Green synthesis of ZnO nanoparticles and its application in the degradation of some dyes. *J. Am. Ceram. Soc.* **2015**, *98*, 1739–1746. https://doi.org/10.1111/jace.13467.
15. Kitture, R.; Koppikar, S.J.; Kaul-Ghanekar, R.; Kale, S.N. Catalyst efficiency, photostability and reusability study of ZnO nanoparticles in visible light for dye degradation. *J. Phys. Chem. Solids* **2011**, *72*, 60–66. https://doi.org/10.1016/j.jpcs.2010.10.090.
16. Zainuri, N.Z.; Hairom, N.H.; Sidik, D.A.; Misdan, N.; Yusof, N.; Mohammad, A.W. Reusability performance of zinc oxide nanoparticles for photocatalytic degradation of POME. *E3S Web Conf.* **2018**, *34*, 02013. https://doi.org/10.1051/e3sconf/20183402013.
17. Sharma, S.; Kumar, K.; Thakur, N.; Chauhan, S.; Chauhan, M.S. The effect of shape and size of ZnO nanoparticles on their antimicrobial and photocatalytic activities: A green approach. *Bull. Mater. Sci.* **2020**, *43*, 20.
18. Small Molecule X-Ray Crystallography, Theory and Workflow. *Encyclopaedia of Spectroscopy and Spectrometry (Second Edition)*, Ed. Le Pevelen, D.D. Elsevier Academic Press, 2010, 2559–2576, doi: 10.1016/B978-0-12-374413-5.00359-6.
19. Zak, K.A.; Abd Majid, W.H.; Abrishami, M.E.; Yousefi, R. X-ray analysis of ZnO nanoparticles by Williamson–Hall and size–strain plot methods. *Solid State Sci.* **2011**, *13*, 251.

20. Lingaraju, K.; Raja Naika, H.; Manjunath, K.; Basavaraj, R.B.; Nagabhushana, H.; Nagaraju, G.; Suresh, D. Biogenic synthesis of zinc oxide nanoparticles using *Ruta graveolens* (L.) and their antibacterial and antioxidant activities. *Appl. Nanosci*. **2016**, *6*, 703.
21. Fuku, X.; Diallo, A.; Maaza, M. Nanoscaled electrocatalytic optically modulated ZnO nanoparticles through green process of *Punica granatum* L. and their antibacterial activities. *Int. J. Electrochem.* **2016**, *2016*, 4682967. https://doi.org/10.1155/2016/4682967.
22. Fuku, X.; Kaviyarasu, K.; Matinise, N.; Maaza, M. Punicalagin green functionalized Cu/Cu2O/ZnO/CuO nanocomposite for potential electrochemical transducer and catalyst. *Nanoscale Res. Lett.* **2016**, *11*, 386. https://doi.org/10.1186/s11671-016-1581-8.
23. Matinise, N.; Fuku, X.G.; Kaviyarasu, K.; Mayedwa, N.; Maaza, M.J. ZnO nanoparticles via Moringa oleifera green synthesis: Physical properties & mechanism of formation. *Appl. Surf. Sci.* **2017**, *406*, 339–347; doi: 10.1016/j.apsusc.2017.01.219.
24. Choudhary, M.K.; Kataria, J.; Sharma, S. Novel Green Biomimetic Approach for Preparation of Highly Stable Au-ZnO Heterojunctions with Enhanced Photocatalytic Activity. *Appl. Nano Mater*. **2018**, *1*, 1870.
25. Suresh, D.; Nethravathi, P.C.; Lingaraju, K.; Rajanaika, H.; Sharma, S.C.; Nagabhushana, H. EGCG assisted green synthesis of ZnO nanopowders: Photodegradative, antimicrobial and antioxidant activities. *Spectrochim. Acta Part A Mol. Biomol. Spectrosc.* **2015**, *136 Pt C*, 1467–1474.
26. Hancock, J.M.; Rankin, W.M.; Hammad, T.M.; Salem, J.S.; Chesnel KHarrison, R.G. Optical and Magnetic Properties of ZnO Nanoparticles Doped with Co, Ni and Mn and Synthesized at Low Temperature. *J. Nanosci. Nanotechnol*. **2015**, *15*, 3809.
27. Akbarian, M.; Mahjoub, S.; Elahi, S.M.; Zabihi, E.; Ebrahim Zabihi, E.; Tashakkorian, H. Green synthesis, formulation and biological evaluation of a novel ZnO nanocarrier loaded with paclitaxel as drug delivery system on MCF-7 cell line. *Colloids Surf. B Biointerface*s **2020**, *186*, 110686.
28. Singh, K.; Singh, J.; Rawat, M. Green synthesis of zinc oxide nanoparticles using Punica Granatum leaf extract and its application towards photocatalytic degradation of Coomassie brilliant blue R-250 dye. *SN Appl. Sci.* **2019**, *1*, 624. https://doi.org/10.1007/s42452-019-0610-5.
29. Otaibi, A.A.; Patil, M.B.; Rajamani, S.B.; Mathad, S.N.; Patil, A.Y.; Amshumali, M.K.; Shaik, J.P.; Asiri, A.M.; Khan, A. Development and Testing of Zinc Oxide Embedded Sulfonated Poly (Vinyl Alcohol) Nanocomposite Membranes for Fuel Cells. *Crystals* **2022**, *12*, 1739. https://doi.org/10.3390/cryst12121739.

crystals

MDPI

Article

Photocatalytic Degradation of Textile Orange 16 Reactive Dye by ZnO Nanoparticles Synthesized via Green Route Using Punica Granatum Leaf Extract

Salma A. Al-Zahrani [1,*], Mallikarjunagouda B. Patil [2,*], Shridhar N. Mathad [3], Arun Y. Patil [4], Ahmed A. Otaibi [1], Najat Masood [1], Dorsaf Mansour [1], Anish Khan [5], A. Manikandan [6] and Edi Syafri [7]

[1] Chemistry Department, Faculty of Science, University of Ha'il, P.O. Box 2440, Ha'il 81451, Saudi Arabia
[2] Bharat Ratna Prof. CNR Rao Research Centre, Basaveshwar Science College, Bagalkot 587101, Karnataka, India
[3] Department of Engineering Physics, K.L.E Institute of Technology, Hubballi 580027, Karnataka, India
[4] School of Mechanical Engineering, KLE Technological University, Vidya Nagar, Hubballi 580031, Karnataka, India
[5] Center of Excellence for Advanced Materials Research, King Abdulaziz University, Jeddah-21589, Saudi Arabia
[6] Department of Chemistry, Bharath Institute of Higher Education and Research (BIHER), Bharath University, Chennai-600073, Tamil Nadu, India
[7] Department of Agricultural Technology, Politeknik Pertanian Negeri Payakumbuh, West Sumatra 26271, Indonesia
* Correspondence: s.alzahrane@uoh.edu.sa (S.A.A.-Z.); mallupatil04@gmail.com (M.B.P.)

Abstract: Since it does not use any dangerous chemicals and is a simple, low-cost process, the green synthesis approach for nanoparticle creation has several benefits compared to the physical and chemical synthesis routes. The current study describes an environmentally friendly synthesis of zinc oxide (ZnO) nanoparticles (NPs) using an extract of *Punica granatum* plant leaves. Fourier-transform infrared spectroscopy (FTIR), ultraviolet-visible spectrophotometer (UV-Vis), field-emission scanning electron microscopy (FESEM), energy-dispersive X-ray spectroscopy, and X-ray diffraction techniques were used to characterize the morphology, composition, and structural properties of the synthesized zinc oxide nanoparticles. The XRD pattern reveals that the ZnO nanoparticles are crystalline and have a diameter of 20 nm. According to the FESEM studies, the ZnO-NPs have sizes ranging from 50 to 100 nm on average and are almost spherical. When exposed to direct sunlight, the produced ZnO-NPs demonstrate impressive photocatalytic oxidation of textile Orange 16, a reactive dye. As a result, our research advances the development of a green photocatalyst for the removal of harmful dyes from water.

Keywords: green synthesis; zinc oxide nanoparticle; photocatalytic; textile Orange 16 reactive dye

Citation: Al-Zahrani, S.A.; Patil, M.B.; Mathad, S.N.; Patil, A.Y.; Otaibi, A.A.; Masood, N.; Mansour, D.; Khan, A.; Manikandan, A.; Syafri, E. Photocatalytic Degradation of Textile Orange 16 Reactive Dye by ZnO Nanoparticles Synthesized via Green Route Using Punica Granatum Leaf Extract. *Crystals* **2023**, *13*, 172. https://doi.org/10.3390/cryst13020172

Academic Editor: Claudia Graiff

Received: 10 December 2022
Revised: 27 December 2022
Accepted: 13 January 2023
Published: 18 January 2023

1. Introduction

New nanoscale materials are being produced as a result of the advancements in nanotechnology. These materials have a variety of uses, including in consumer goods, nanomedicine, and nanoelectronics [1,2]. Because of their superior chemical and physical characteristics when compared to their bulk counterparts, research on such materials has increased significantly in recent years. Metal oxide nanostructures have been created, and they have a variety of uses in various industries. A semiconductor with a greater band gap (3.4 eV) is zinc oxide (ZnO). Applications for it include dye degradation, gas sensors, solar cells, and many others [3]. Numerous chemical and physical techniques, such as the sol–gel technique [4], the precipitation method [5], the arc discharge technique [6], the hydrothermal method [7], and the laser ablation method [8], have been adopted for the synthesis of ZnO nanoparticles. Due to its numerous advantages over the physical and

chemical approaches—including the fact that it does not use dangerous chemicals and is both environmentally friendly and economically advantageous—synthesis via the green method has been used to prepare ZnO nanoparticles [9,10]. This approach makes use of biological components that are readily available from plants.

Because they are readily available, leaves from the *Punica grantum* plant have been employed. The family of *Punicaceae*, which consists of two different species, is dominated by the pomegranate species (Punica granatum). *Punica grantum* plant leaves contain alkaloids, tannins, triterpenic acids, and flavonoids as phytochemicals [11]. Utilizing chemical reduction, these phytoconstituents produce metal oxide nanoparticles by acting as the stabilizing and reducing agents. As far as we are aware, there has not been any research on the usage of *P. granatum* leaves in the preparation of ZnO-NPs.

Organic substances called dyes are used in the paper, food, leather, and textile industries. Strongly colored, hazardous dyes are present in the effluents from these enterprises. The discharged effluents will enter running water, polluting the surface and groundwater and perhaps endangering the health of aquatic life as well as that of people, fauna, and the environment. Before release, the effluents would be treated to break down the dye into non-toxic species. Different purification methods, including chemical, biological, and physical techniques, have been developed, depending on the type of pollution. ZnO-NPs have been used to degrade dyes with success [12–14]. Through catalytic photooxidation with ZnO-NPs, reactive oxidative hydroxide radicals are created, which destroy the dyes. According to its chemical makeup, the textile Orange 16 reactive dye is an organic substance classified as a disulfonated triphenylmethane dye. Although originally designed for the textile industry, it is now frequently used for protein staining in biochemistry. The catalyst should be stable and reusable in addition to having a high degradation efficiency, as these qualities are crucial for industrial applications. Numerous investigations [15,16] have shown that ZnO-NPs are stable and reusable.

The *P. granatum* leaf extract was used in the current work's green synthesis to create ZnO-NPs. Under exposure to direct sunlight, the green ZnO-NPs that were generated were used to photocatalytically degrade the textile Orange 16 reactive dye.

2. Materials and Methodology

2.1. Materials

We gathered *Punica granatum* leaves from a field in Kaladagi near Bagalkot (India). Zinc nitrate hexahydrate of high purity was procured from Sigma-Aldrich, Mumbai, India. All water used in the experiment was deionized distilled water. We bought textile Orange 16 reactive dye from a local market in Bagalkot, Karnataka, India, through a textile business. None of the chemicals were further purified before use. Glassware washed in a prepared Piranha solution (3:1 volume ratio of H_2SO_4/H_2O_2) was rinsed with deionized (DI) water with a resistivity of 16.4 MΩ·cm (millipore water), dried in an oven, and returned for later use.

2.2. Methodology

2.2.1. Extraction of *Punica granatum* Leaf

Young *P. granatum* leaves were collected from a *Punica granatum* plantation at a Kaladagi village near Bagalkot (India). The leaves' middle rib was cut off. The leaves that remained were cleaned with distilled water to get rid of dust, and they were then dried in the shade to get rid of all the moisture. An aqueous extract of *Punica granatum* leaf was prepared. During the process, the dried leaves were weighed accurately and were finely grounded in a mixture. Then, deionized water was added to the dried fine powder. For about three hours, the mixture was refluxed at 60 °C, using the Soxhlet extractor apparatus. Once the green color turned brownish, the process was stopped. At room temperature, the solution was allowed to cool for the period of ten to fifteen minutes. Furthermore, Whatman No. 41 filter paper was used to filter the solution, and the filtrate was then

collected in a dry flask while the residue was thrown away. For future use, the leaf extract was kept at ambient temperature.

2.2.2. Green Synthesis of Zinc Oxide Nanoparticles (ZnO-NPs)

In deionized water, a solution of $Zn(NO_3)_2 \cdot 6H_2O$ (0.1 M) was made. The mixture was made homogeneously by stirring it without being heated. After that, a magnetic stirrer was used to gradually add drops of the aqueous leaf extract to the zinc nitrate solution. After the leaf extract was completely added, the resulting mixture was stirred with heating at 60 °C for 3–4 h on a hot plate until it took the form of slurry. The obtained slurry substance was filtered and placed in a crucible. The sample was calcined at 500 °C in a muffle furnace at a heating rate of 5 °C for 5 h. After calcination, white powder was obtained and stored properly.

2.2.3. Characterization of ZnO-NPs

A Siemens D 5000 (Malvern, UK) powder X-ray diffractometer was used to perform X-ray diffraction on the powdered zinc oxide nanoparticles. The UV-visible spectrum of the zinc oxide nanoparticles was recorded by employing a UV spectrophotometer (Systonic, Bangalore, India). The samples were evaluated between 200 and 800 nm. A Shimadzu (Model: IR Affinity-1, Tokyo, Japan) FTIR spectrometer was used to perform Fourier-transform spectroscopic measurements. A Carl Zeiss (Model: Sigma 300, Bangalore, India) field-emission scanning electron microscope (FESEM) was used to examine the surface morphology and the dimension of the particles of the prepared ZnO nanoparticles. The Oxford instrument (Buckinghamshire, UK), an energy-dispersive X-ray spectroscopy (EDX), was used to obtain the spectrum to check the purity of the synthesized ZnO nanoparticles and the stoichiometry of the samples. The particle size of the synthesized ZnO-NPs was determined using the Zetasizer (Model 3000HS, Malvern, UK). On a cuvette, the zeta average size of ZnO-NPs suspended in DI water was determined. The measurement was repeated three times, and the average value was used for data analysis.

2.2.4. Photocatalytic Activity of ZnO-NPs

A photodegradation study of textile Orange 16 reactive dye in water by exposure to sunlight was used to determine the ZnO nanoparticles as the photocatalysts. For this, an artificial, laboratory-simulated dye was prepared by dissolving the dye in water until the solution's absorbance value was more than one, i.e., 0.4 g in 100 mL of water. To the prepared colored mixture, a known amount of ZnO (i.e., 0.1 g), which would act as a photocatalyst, was added. Later, the aqueous solution was sonicated for 30 min. The solution was then kept in sunlight while being constantly stirred. After 30 min, 5 mL of the solution was withdrawn and centrifuged to settle down the ZnO photocatalyst. The supernatant solution was used to measure the absorbance with a UV-Vis spectrophotometer. From the experiment, it was observed that the value of absorbance reduced after each interval, showing the degradation of the dye by the ZnO-NPs. The detailed stepwise green synthesis of ZnO nanoparticles and their photocatalytic action are shown in Figure 1.

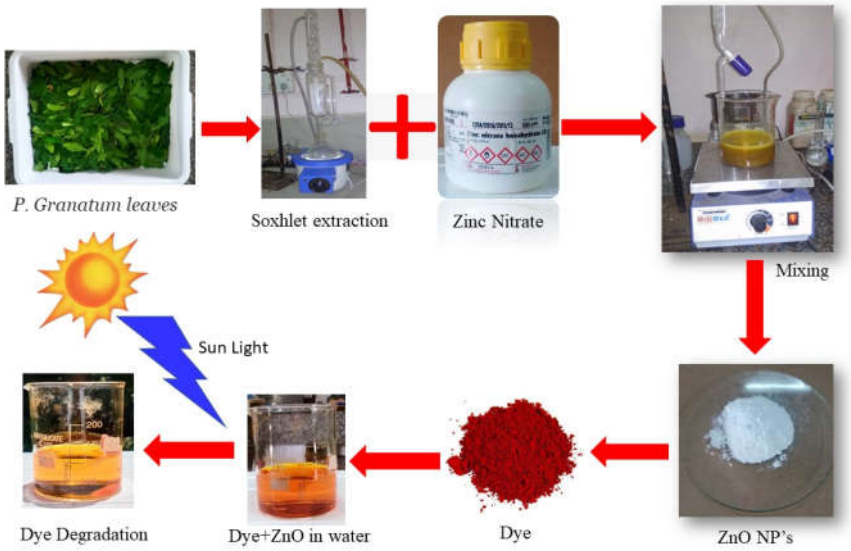

Figure 1. Step-by-step process of ZnO-NP synthesis via green route and the degradation of the dye.

3. Results and Discussion

3.1. X-ray Diffraction Analysis

Figure 2 depicts the X-Ray diffraction graph of the green synthesized ZnO nanoparticles. The sample was examined at various angles, ranging from 0° to 70°. ZnO nanoparticles have significant peaks at 2θ = 31.81°, 34.49°, 36.28°, 47.62°, 56.63°, 62.91°, and 68°, which can be designated as (100), (002), (101), (102), (110), (103), and (200), respectively. The orientation and crystallinity of the ZnO-NPs were revealed by using the X-ray pattern. The JCPDS data sheet/ICDD no. 36-1451 was used to compute the XRD pattern. The obtained X-ray pattern demonstrate that ZnO-NPs were synthesized using the green synthesis route, with the establishment of crystalline and wurtzite hexagonal structures. The particle dimension of ZnO-NPs was computed using the Debye–Scherrer equation from the highest peak (101) in the XRD graph:

$$d = \frac{K\lambda}{\beta cos\theta} \quad (1)$$

where d is the size of the crystallite; λ is the wavelength for diffraction; β is the corrected value of FWHM; θ is the angle of diffraction; and K is the universal and its value is near unity, i.e., 0.94.

The purity of the ZnO-NPs is confirmed by the absence of diffraction peaks from other phases.

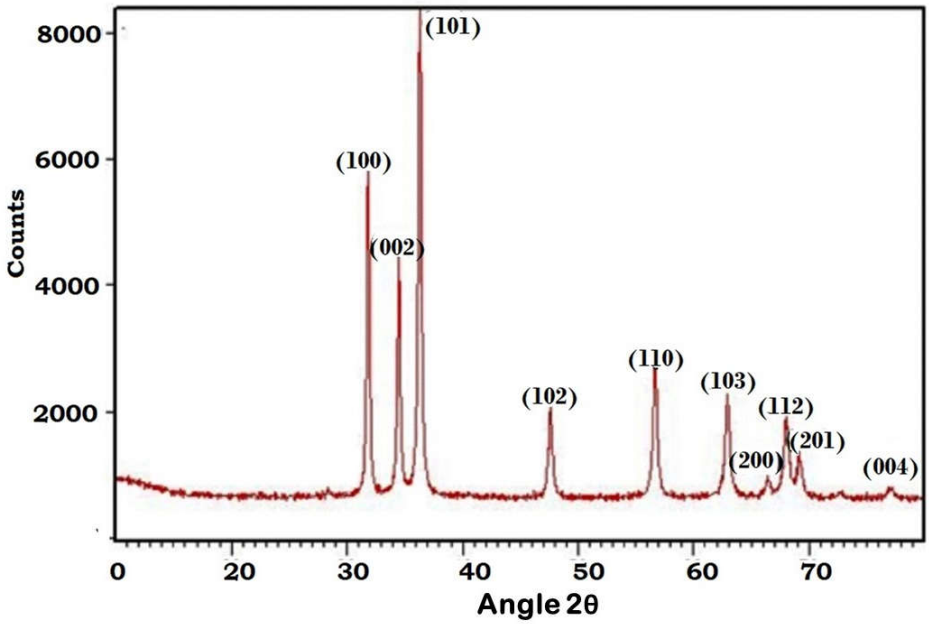

Figure 2. X-ray diffraction curves of green synthesized ZnO nanoparticles.

Bragg's equations 3-5 were used to calculate the inter-planar spacing (d), the lattice parameters (a = b and c) for the hexagonal wurtzite structure, and the volume of the hexagonal system unit cell (V) [17–20]. Table 1 summarizes all of these parameters.

$$n\lambda = 2d\ sin\ \theta \quad (2)$$

$$\frac{1}{d_{hkl}^2} = \frac{4}{3}\left(\frac{h^2 + hk + k^2}{a^2}\right) + \frac{l^2}{c^2} \quad (3)$$

$$V = \frac{\sqrt{3}}{2}a^2c \quad (4)$$

where d_{hkl} = inter-planar spacing; V = volume of the unit cell; and a, c = lattice parameters for the ZnO-NP.

Table 1. Crystallite size (D), inter-planar spacing (d), lattice parameters ($a = b$ and c), and volume (V) were calculated from the XRD measurements at 50 mmol/kg concentrations of $Zn(NO_3)_2{\cdot}6H_2O$.

[a]m (mmol/kg)	D (nm)	d (nm)	$a = b$ (nm)	c (nm)	V (nm^3)
50	31.158	0.256	0.325	0.527	4.721

[a]m represents the molality of $Zn(NO_3)_2{\cdot}6H_2O$ in water.

3.2. Particle Size Analysis

The particle size of the ZnO-NPs is depicted in Figure 3. The obtained results reveal that the size of ZnO particles ranges between 60 and 100 nm. The average particle size is measured at 80 nm.

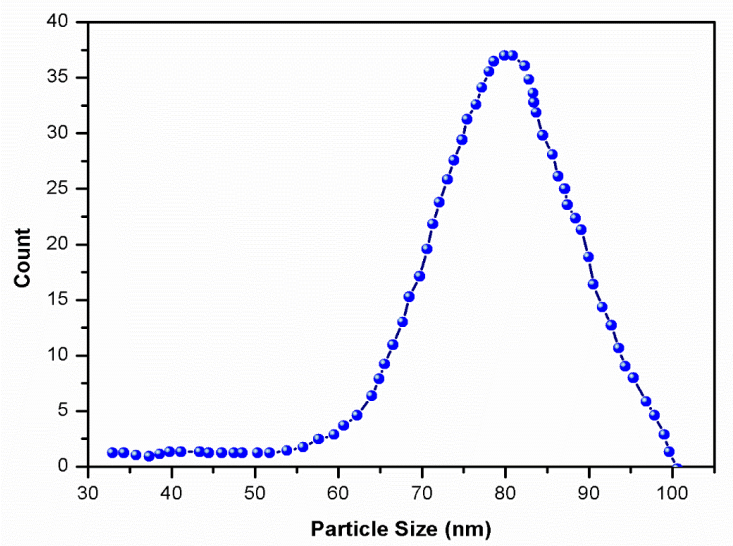

Figure 3. Histogram of ZnO particle size distribution.

3.3. UV-Visible Spectroscopic Analysis

Surface plasmon resonance distinguishes the absorbance pattern of nanoparticles from that of their bulk counterparts. The UV-visible measurement was used to confirm the formation of nanoparticles. Figure 4 depicts the UV-visible absorption spectrum of the ZnO-NPs. Using a systonic UV spectrophotometer, the substance was analyzed between 200 and 800 nm. The color of a solution of zinc nitrate hexahydrate ($Zn(NO_3)_2H_2O$) changed from white to brown when the *P. granatum* leaf extract was added. This resulted from the solution's synthesis of ZnO-NPs. The nanoparticles of zinc oxide are responsible for stimulating the surface plasmon vibrations, which in turn generate color changes. The absorbance peak was found to be centered at 382 nm, indicating that zinc nitrate hexahydrate had been converted to ZnO-NPs [21–23].

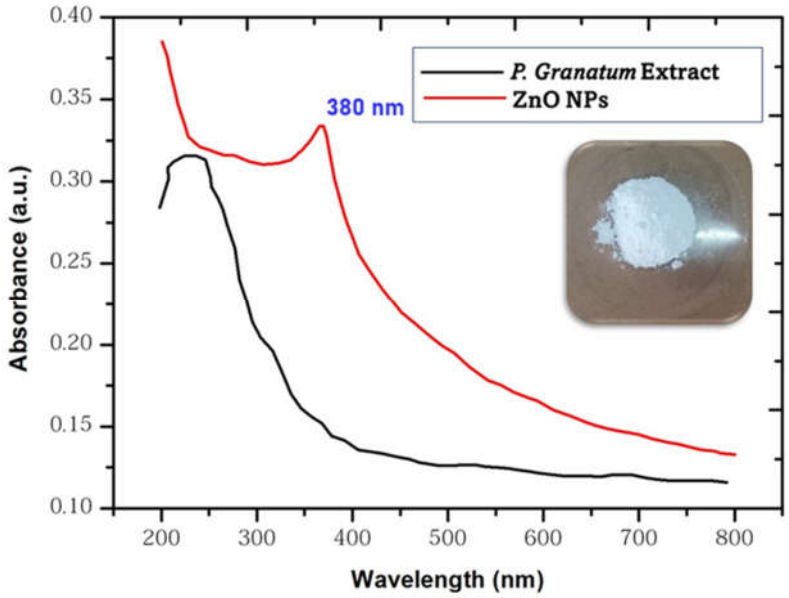

Figure 4. ZnO-NPs and *P. granatum* leave extract spectra measured using an UV-visible spectrophotometer. (Inside: photograph of ZnO-NPs synthesized via green method).

The optical energy band gap (E_g) was calculated using Formula (5), and the results are shown in Table 2.

$$E_g = \frac{hc}{\lambda} \quad (5)$$

From this formula, 'h' represents the Planck's constant (6.626×10^{-34} J s), 'c' corresponds to the velocity of light (the value is 3×10^8 m s^{-1}), and λ corresponds to the wavelength of the peak with the maximum intensity [24].

Table 2. λmax and energy band gap (E_g) results of ZnO-NPs at three different concentrations of zinc nitrate hexahydrate.

[a]**m (mmpl/kg)**	λ_{max} **(nm)**	E_g **(eV)**
5	381	3.436 ± 0.3
10	386	3.369 ± 0.4
50	390	3.361 ± 0.3

[a]m represents the molality of $Zn(NO_3)_2 \cdot 6H_2O$ in water.

The band gap values were calculated, and the results are nearly equivalent to 3.4 eV, which is consistent with previously reported values in the literature. Suresh et al. (3.33 eV) [25] and Hancock et al. (3.39 eV) [26] reported comparable band gap results. The variation in the shape and size of the ZnO-NPs may explain the difference in E_g with Zn $(NO_3)_2 \cdot 6H_2O$ concentration. In addition, a decrease in E_g values is attributed to an increase in ZnO particle size [27].

3.4. FESEM and EDX Analysis

ZnO may be produced into several nanostructures, including nanospheres, nanorods, and others. By looking at and analyzing each minute topographical feature using a field-emission scanning electron microscope (FESEM), the particle size and shape may be determined. The particle size and shape of the synthesized ZnO nanoparticles were analyzed with the aid of a Carl Zeiss FESEM. Figure 5 displays a FESEM picture of the ZnO nanoparticles that were synthesized via the green route. This image demonstrates that the particle is composed of nanostructures, which are even smaller structures. The XRD investigation indicated that the nanoparticles are fully spherical, with an average diameter of 80 nm.

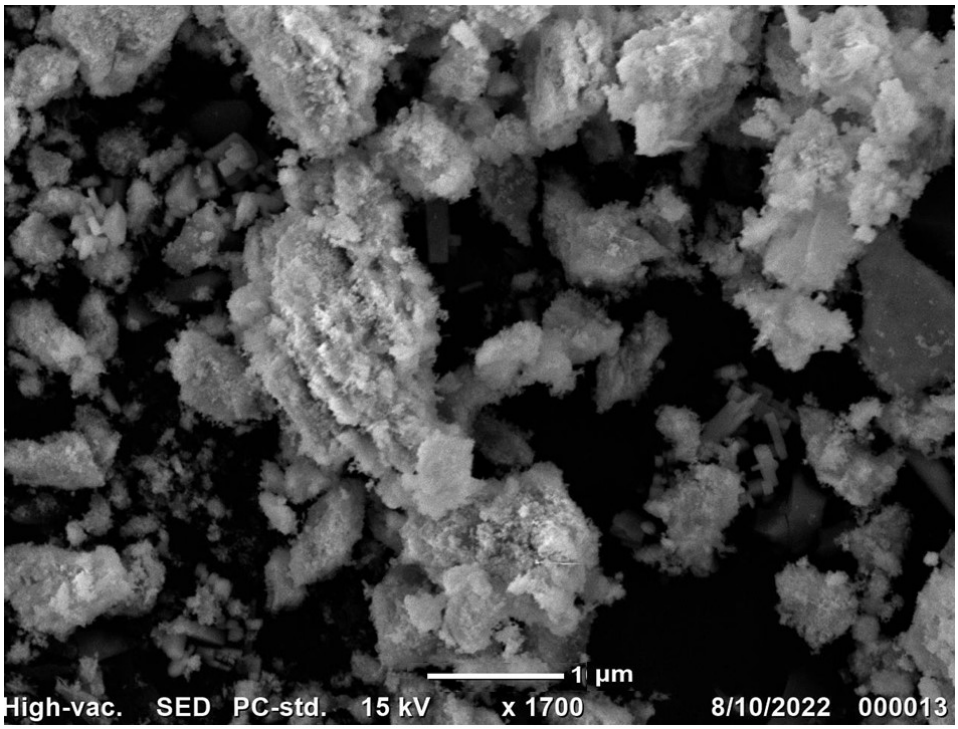

Figure 5. FESEM picture of zinc oxide NPs synthesized via the green route.

EDX was utilized to undertake an elemental investigation or chemical composition on the ZnO nanoparticles made in an environmentally responsible manner. The stoichiometry and chemical purity of the samples were analyzed using an EDX-equipped equipment from Oxford. The EDX spectrum of the ZnO nanoparticles is illustrated here in Figure 6. The EDX spectrum indicates indisputably that ZnO and oxygen (O) ions are present in the ZnO nanoparticles formed by the *P. Granatum* reaction. According to the findings of the elemental analysis, the ZnO powder is made up of 76% zinc and 15% oxygen, which shows that it is quite pure and only comprises a minor number of contaminants. The stoichiometry reveals that the mass percentages of zinc and oxygen should be 80.3% and 19.7%, respectively, if we are to trust the formulae.

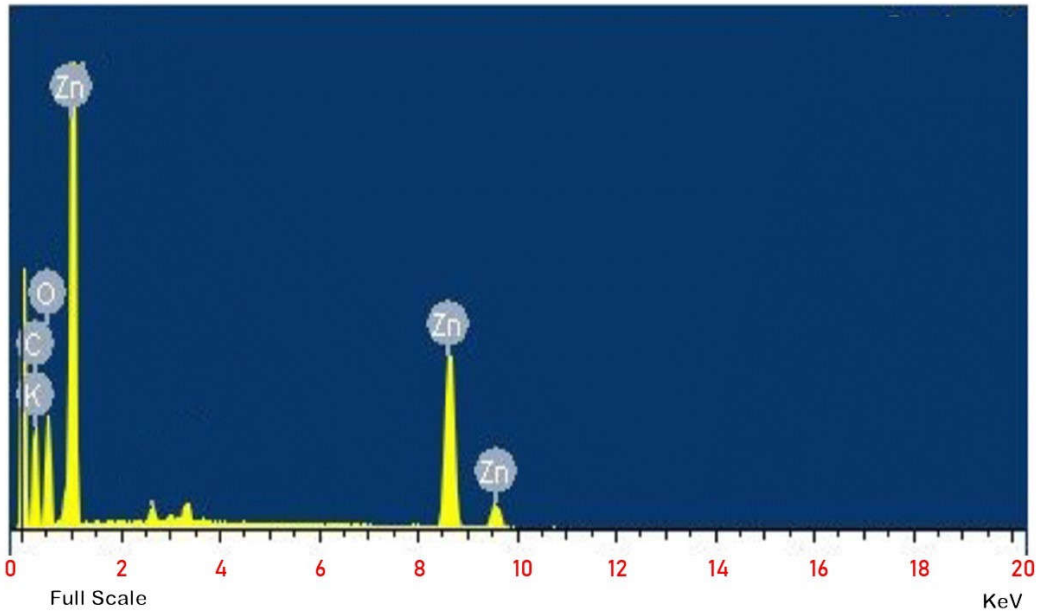

Figure 6. EDAX pattern for the green synthesized ZnO-NPs (Zn—zinc, O—oxygen, and C—carbon).

3.5. FT-IR Analysis

FT-IR spectroscopy was used to establish the presence of the Zn–O bond and its formation mechanism, as well as to detect the photo components that coat the surface of the ZnO-NPs. Fourier-transform infrared spectroscopy was performed using a Bruker Alpha FTIR as the instrument. Figure 7 depicts the FT-IR spectra of the ZnO-NPs that were synthetically generated via the green route. Both the 3610 cm^{-1} and 3822 cm^{-1} spectral peaks are the consequence of O–H stretching. The C–H stretch is responsible for the peak that appears at roughly 2354 cm^{-1}. The peak is induced by C=O stretching and is located at about 1512 cm^{-1}. There is a link between the peaks at 1635 cm^{-1} and ZnO vibrations caused by bending deformation. At 610 cm^{-1}, strong vibrational bands are produced as a result of the stretching modes utilized to form the ZnO nanoparticles. The phytoconstituents of P. granatum prevent the aggregation of ZnO-NPs during their production [22,23,28,29]. This is achieved by stabilizing the nanoparticles' surface.

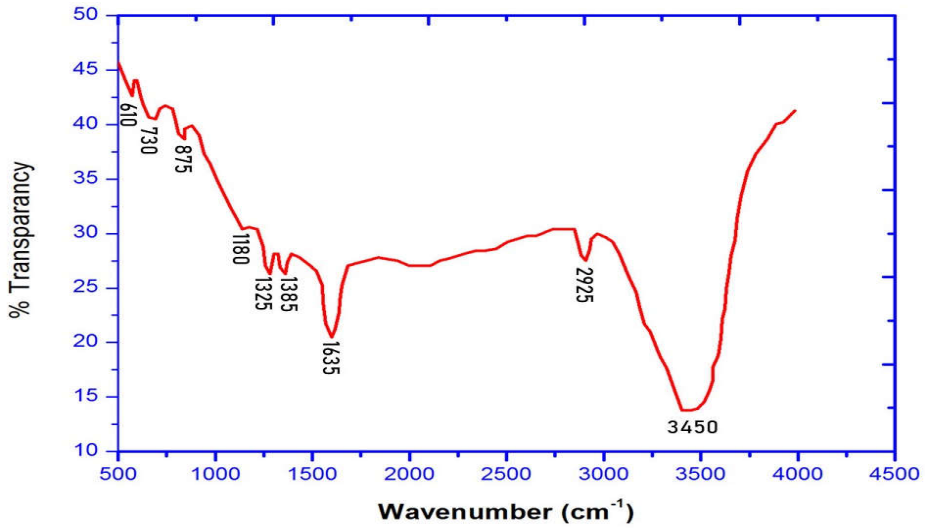

Figure 7. FTIR spectrum of ZnO-NPs.

3.6. Photocatalytic Activity

To evaluate the photodegradation of textile Orange 16 reactive dye in the presence of ZnO nanoparticles, the decrease in the absorbance of the dye was determined. The decrease in the absorbance of the dye solution as a function of exposure length is consistent with a decline in the concentration of textile Orange 16 reactive dye. Over time, the concentration of the blue pigment in the dye solution progressively lost its vibrancy, until it ultimately became light blue. Figure 8 depicts the deterioration of the textile Orange 16 reactive dye stain as a function of time in the samples exposed to sunlight. It can be seen that 600 nm is the wavelength at which textile Orange 16 reactive dye has the highest absorption peak. In addition, it reveals that ZnO-NPs are capable of significantly reducing the pollutant within three hours.

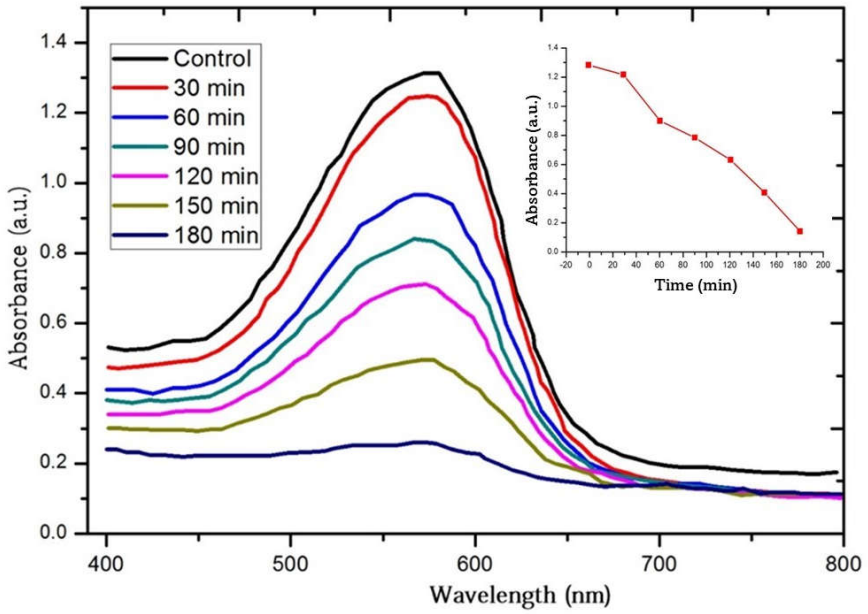

Figure 8. UV-vis absorption spectra showing the degradation of textile Orange 16 reactive dye by photocatalytic action using zinc oxide NPs synthesized via the green route at 30 min time intermissions. Inset: decrease in intensity of textile Orange 16 reactive dye in the presence of ZnO-NPs with time.

3.7. Recyclability and Photostability

Three cycles of photocatalysis were conducted to assess whether or not the photocatalyst could be recycled. The images are depicted in Figure 9. Figure 9a shows a 100% efficiency even after three cycles of photocatalysis. In addition, as seen in Figure 9b, the XRD measurements performed after the photocatalytic phenomenon show that the crystalline structure of ZnO has not altered when compared to before the photocatalytic process was undertaken.

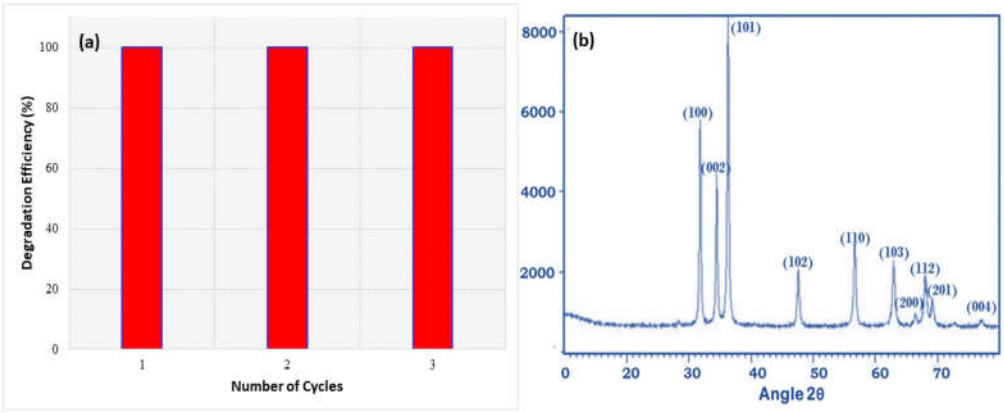

Figure 9. (**a**) The degradation profile of ZnO-NPs for three cycles and (**b**) XRD of ZnO after three cycles.

Figure 10 shows the photodegradation of the Orange 16 dye by using green synthesized ZnO nanoparticles. As observed in Figure 10, the effectiveness of the ZnO-NPs as photocatalysts for the breakdown of organic materials is shown by the decline in the color intensity of the dye with respect to the time of exposure to sunlight.

Figure 10. The color intensity before and after photodegradation using green synthesized ZnO nanoparticles.

3.8. Photolysis

There are three types of photocatalytic dye degradation mechanisms: (1) dye sensitization via charge injection, (2) indirect dye degradation via oxidation/reduction, and (3) direct photolysis of the dye. Photocatalytic substances are generally classified into three generations. One-component (e.g., ZnO and TiO_2) and multi-component semiconductor metal oxide (e.g., ZnO-TiO_2 and Bi_2O_3-ZnO) photocatalysts are classified as first-generation and second-generation, respectively. Third-generation photocatalysts are photocatalysts that are dispersed on an inert solid substrate (e.g., Ag-Al_2O_3 and ZnO-C).

Because some dyes are degraded by direct UV irradiation, it is necessary to investigate the extent to which textile Orange 16 reactive dye is photolyzed in the absence of a photocatalyst. In the absence of the photocatalyst, direct UV radiation exposure photolyzed textile Orange 16 reactive dye by up to 25% in 30 min. When ZnO-NPs were used as a photocatalyst and exposed to UV radiation, it was discovered that the

photodegradation of the dye increased by decolorizing the textile Orange 16 reactive dye with an efficiency of 96% in 30 min. The time-dependent photocatalytic degradation and the photolysis of textile Orange 16 reactive dye concentration are shown in Figure 11.

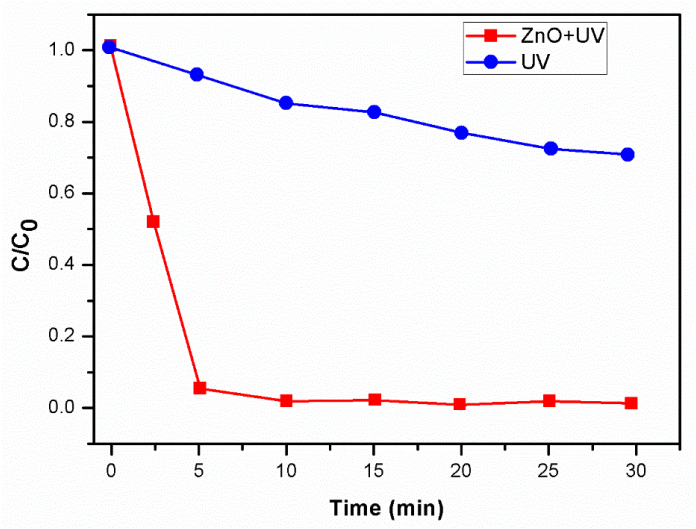

Figure 11. Time-dependent photocatalytic degradation and photolysis of textile Orange 16 reactive dye concentration (C/C_0).

3.9. Comparison

The dye photodegradation in the presence of the synthesized ZnO-NPs was compared to a commercial ZnO and previously reported work. The results are tabulated in Table 3.

Table 3. Comparison of ZnO-NPs as a photocatalyst for dye degradation.

Sl. No	Photocatalyst	Time (min)	% Photocatalytic Degradation of Dye	Reference
1	ZnO	180	94	Present work
2	ZnO	180	95	Commercial ZnO
3	ZnO	160	86.9	[17]

Among the tested ZnO NPs, commercial ZnO performed the best when compared to other ZnO NPs.

4. Conclusions

In the current investigation, an extract of the leaves of *P. granatum* was dissolved in water and utilized in a green synthesis process, which resulted in the successful generation of ZnO-NPs. The preparation of spherical, polydisperse ZnO-NPs with sizes ranging from 50 to 100 nm and an average size of 80 nm was performed. The majority of the nanoparticles are spherical and have an 80 nm diameter. According to the results of the EDX analysis, the ZnO powder has a very high degree of purity and includes nearly no impurities. The powder consists of 76% zinc and 15% oxygen. According to the results of the photocatalytic experiment, the bio-produced ZnO-NPs are able to photodegrade the textile Orange 16 reactive dye with an overall efficiency of 93%. The photolysis of the textile Orange 16 reactive dye concentration without and with ZnO-NPs shows that the ZnO-NPs play the role of photocatalysts effectively. According to the results of this work, the manufacture of ZnO-NPs using the *P. granatum* leaf extract is safe, inexpensive,

straightforward, and environmentally friendly, and these nanoparticles have shown efficacy as green photocatalysts in the actual treatment of wastewater.

Author Contributions: Conceptualization, S.A.A.-Z. and M.B.P.; methodology, S.N.M. and A.Y.P.; software, A.A.O; validation, N.M., D.M. and A.K.; formal analysis, A.M.; investigation, E.S.; project administration, S.A.A.-Z. All authors have read and agreed to the published version of the manuscript.

Funding: This research has been funded by Scientific Research Deanship at the University of Ha'il-Saudi Arabia through project number RG-21 032.

Data Availability Statement: Data can be provided on the request from the corresponding author.

Acknowledgments: Author are thankful for VGST, Bangalore, India for the support.

Conflicts of Interest: The authors declare no conflict of interest.

References

1. Saini, R.; Saini, S.; Sharma, S. Nanotechnology: The future medicine. *J. Cutan. Aesthetic Surg.* **2010**, *3*, 32. https://doi.org/10.4103/0974-2077.63301.
2. Singh, A. Synthesis, characterization, electrical and sensing properties of ZnO nanoparticles. *Adv. Powder Technol.* **2010**, *21*, 609–613.
3. Nohavica, D.; Gladkov, P. ZnO nanoparticles and their applications—New achievments. *NANOCON* **2010,** *1,* 121–124. https://doi.org/10.1016/j.cej.2012.01.076.
4. Azlina, H.N.; Hasnidawani, J.N.; Norita, H.; Surip, S.N. Synthesis of SiO_2 nanostructures using sol-gel method. *Acta Phys. Pol. A* **2016**, *129*, 842–844.
5. Raoufi, D. Synthesis and microstructural properties of ZnO nanoparticles prepared by precipitation method. *Renew Energy* **2013**, *50*, 932–937. https://doi.org/10.1016/j.renene.2012.08.076.
6. Ashkarran, A.A.; Irajizad, A.; Mahdavi, S.M.; Ahadian, M.M. ZnO nanoparticles prepared by electrical arc discharge method in water. *Mater. Chem. Phys.* **2009**, *118*, 6–8. https://doi.org/10.1016/j.matchemphys.2009.07.002.
7. Aneesh, P.M.; Vanaja, K.A.; Jayaraj, M.K. Synthesis of ZnO nanoparticles by hydrothermal method. In *Nanophotonic Materials IV*; SPIE: Bellingham, WA, USA, 2007.
8. Singh, S.C.; Gopal, R. Synthesis of colloidal zinc oxide nanoparticles by pulsed laser ablation in aqueous media. *Phys. E Low-Dimens. Syst. Nanostructures* **2008**, *40*, 724–730. https://doi.org/10.1016/j.physe.2007.08.155.
9. Singh, J.; Kumar, S.; Alok, A.; Upadhyay, S.K.; Rawat, M.; Tsang, D.C.; Bolan, N.; Kim, K.H. The potential of green synthesized zinc oxide nanoparticles as nutrient source for plant growth. *J. Clean. Prod.* **2019**, *214*, 1061–1070. https://doi.org/10.1016/j.jclepro.2019.01.018.
10. Singh, J.; Dutta, T.; Kim, K.H.; Rawat, M.; Samddar, P.; Kumar, P. 'Green' synthesis of metals and their oxide nanoparticles: Applications for environmental remediation. *J. Nanobiotechnol.* **2018**, *16*, 84. https://doi.org/10.1186/s12951-018-0408-4.
11. Wang, R.; Ding, Y.; Liu, R.; Xiang, L.; Du, L. Pomegranate: Constituents, bioactivities and pharmacokinetics. *Fruit Veg. Cereal Sci. Biotechnol.* **2010**, *4*, 77–87.
12. Hassan, S.S.M.; Azab, W.I.M.E.; Ali, H.R.; Mansour, M.S.M. Green synthesis and characterization of ZnO nanoparticles for photocatalytic degradation of anthracene. *Adv. Nat. Sci. Nanosci. Nanotechnol.* **2015**, *6*, 045012. https://doi.org/10.1088/2043-6262/6/4/045012.
13. Bhuyan, T.; Mishra, K.; Khanuja, M.; Prasad, R.; Varma, A. Biosynthesis of zinc oxide nanoparticles from Azadirachta indica for antibacterial and photocatalytic applications. *Mater. Sci. Semicond. Process.* **2015**, *32*, 55–61. https://doi.org/10.1016/j.mssp.2014.12.053.
14. Davar, F.; Majedi, A.; Mirzaei, A. (2015) Green synthesis of ZnO nanoparticles and its application in the degradation of some dyes. *J. Am. Ceram. Soc.* **2015**, *98*, 1739–1746. https://doi.org/10.1111/jace.13467.
15. Kitture, R.; Koppikar, S.J.; Kaul-Ghanekar, R.; Kale, S.N. Catalyst efficiency, photostability and reusability study of ZnO nanoparticles in visible light for dye degradation. *J. Phys. Chem. Solids* **2011**, *72*, 60–66. https://doi.org/10.1016/j.jpcs.2010.10.090.
16. Zainuri, N.Z.; Hairom, N.H.; Sidik, D.A.; Misdan, N.; Yusof, N.; Mohammad, A.W. Reusability performance of zinc oxide nanoparticles for photocatalytic degradation of POME. *E3S Web Conf.* **2018**, *34*, 02013. https://doi.org/10.1051/e3sconf/20183402013.
17. Sharma, S.; Kumar, K.; Thakur, N.; Chauhan, S.; Chauhan, M.S. The effect of shape and size of ZnO nanoparticles on their antimicrobial and photocatalytic activities: A green approach. *Bull. Mater. Sci.* **2020**, *43*, 20.
18. Small Molecule X-Ray Crystallography, Theory and Workflow. *Encyclopaedia of Spectroscopy and Spectrometry (Second Edition)*, Ed. Le Pevelen, D.D. Elsevier Academic Press, 2010, 2559–2576, doi: 10.1016/B978-0-12-374413-5.00359-6.
19. Zak, K.A.; Abd Majid, W.H.; Abrishami, M.E.; Yousefi, R. X-ray analysis of ZnO nanoparticles by Williamson–Hall and size–strain plot methods. *Solid State Sci.* **2011**, *13*, 251.

20. Lingaraju, K.; Raja Naika, H.; Manjunath, K.; Basavaraj, R.B.; Nagabhushana, H.; Nagaraju, G.; Suresh, D. Biogenic synthesis of zinc oxide nanoparticles using *Ruta graveolens* (L.) and their antibacterial and antioxidant activities. *Appl. Nanosci*. **2016**, *6*, 703.
21. Fuku, X.; Diallo, A.; Maaza, M. Nanoscaled electrocatalytic optically modulated ZnO nanoparticles through green process of *Punica granatum* L. and their antibacterial activities. *Int. J. Electrochem.* **2016**, *2016*, 4682967. https://doi.org/10.1155/2016/4682967.
22. Fuku, X.; Kaviyarasu, K.; Matinise, N.; Maaza, M. Punicalagin green functionalized Cu/Cu2O/ZnO/CuO nanocomposite for potential electrochemical transducer and catalyst. *Nanoscale Res. Lett.* **2016**, *11*, 386. https://doi.org/10.1186/s11671-016-1581-8.
23. Matinise, N.; Fuku, X.G.; Kaviyarasu, K.; Mayedwa, N.; Maaza, M.J. ZnO nanoparticles via Moringa oleifera green synthesis: Physical properties & mechanism of formation. *Appl. Surf. Sci.* **2017**, *406*, 339–347; doi: 10.1016/j.apsusc.2017.01.219.
24. Choudhary, M.K.; Kataria, J.; Sharma, S. Novel Green Biomimetic Approach for Preparation of Highly Stable Au-ZnO Heterojunctions with Enhanced Photocatalytic Activity. *Appl. Nano Mater*. **2018**, *1*, 1870.
25. Suresh, D.; Nethravathi, P.C.; Lingaraju, K.; Rajanaika, H.; Sharma, S.C.; Nagabhushana, H. EGCG assisted green synthesis of ZnO nanopowders: Photodegradative, antimicrobial and antioxidant activities. *Spectrochim. Acta Part A Mol. Biomol. Spectrosc.* **2015**, *136 Pt C*, 1467–1474.
26. Hancock, J.M.; Rankin, W.M.; Hammad, T.M.; Salem, J.S.; Chesnel KHarrison, R.G. Optical and Magnetic Properties of ZnO Nanoparticles Doped with Co, Ni and Mn and Synthesized at Low Temperature. *J. Nanosci. Nanotechnol*. **2015**, *15*, 3809.
27. Akbarian, M.; Mahjoub, S.; Elahi, S.M.; Zabihi, E.; Ebrahim Zabihi, E.; Tashakkorian, H. Green synthesis, formulation and biological evaluation of a novel ZnO nanocarrier loaded with paclitaxel as drug delivery system on MCF-7 cell line. *Colloids Surf. B Biointerface*s **2020**, *186*, 110686.
28. Singh, K.; Singh, J.; Rawat, M. Green synthesis of zinc oxide nanoparticles using Punica Granatum leaf extract and its application towards photocatalytic degradation of Coomassie brilliant blue R-250 dye. *SN Appl. Sci.* **2019**, *1*, 624. https://doi.org/10.1007/s42452-019-0610-5.
29. Otaibi, A.A.; Patil, M.B.; Rajamani, S.B.; Mathad, S.N.; Patil, A.Y.; Amshumali, M.K.; Shaik, J.P.; Asiri, A.M.; Khan, A. Development and Testing of Zinc Oxide Embedded Sulfonated Poly (Vinyl Alcohol) Nanocomposite Membranes for Fuel Cells. *Crystals* **2022**, *12*, 1739. https://doi.org/10.3390/cryst12121739.